⌘ *Author's Choice*

THE JOURNAL OF BIOLOGICAL CHEMISTRY VOL. 285, NO. 12, pp. 8743–8758, March 19, 2010

Mechano-transduction in Osteoblastic Cells Involves Strain-regulated Estrogen Receptor α-mediated Control of Insulin-like Growth Factor (IGF) I Receptor Sensitivity to Ambient IGF, Leading to Phosphatidylinositol 3-Kinase/AKT-dependent Wnt/LRP5 Receptor-independent Activation of β-Catenin Signaling*

Received for publication, June 2, 2009, and in revised form, November 23, 2009 Published, JBC Papers in Press, December 30, 2009, DOI 10.1074/jbc.M109.027086

Andrew Sunters[‡1], Victoria J. Armstrong[‡], Gul Zaman[‡], Robert M. Kypta[§¶], Yoshiaki Kawano[§], Lance E. Lanyon[‡], and Joanna S. Price[‡]

From the [‡]Department of Veterinary Basic Sciences, Royal Veterinary College, Royal College Street, London NW1 0TU, United Kingdom, the [§]Department of Oncology, Imperial College London, London W12 0NN, United Kingdom, and the [¶]Centre for Cooperative Research in Biosciences, CIC bioGUNE, 48160 Derio, Spain

The capacity of bones to adjust their mass and architecture to withstand the loads of everyday activity derives from the ability of their resident cells to respond appropriately to the strains engendered. To elucidate the mechanisms of strain responsiveness in bone cells, we investigated *in vitro* the responses of primary mouse osteoblasts and UMR-106 osteoblast-like cells to a single period of dynamic strain. This stimulates a cascade of events, including activation of insulin-like growth factor I receptor (IGF-IR), phosphatidylinositol 3-kinase-mediated phosphorylation of AKT, inhibition of GSK-3β, increased activation of β-catenin, and associated lymphoid-enhancing factor/T cell factor-mediated transcription. Initiation of this pathway does not involve the Wnt/LRP5/Frizzled receptor and does not culminate in increased IGF transcription. The effect of strain on IGF-IR is mimicked by exogenous des-(1–3)IGF-I and is blocked by the IGF-IR inhibitor H1356. Inhibition of strain-related prostanoid and nitric oxide production inhibits strain-related (and basal) AKT activity, but their separate ectopic administration does not mimic it. Strain-related IGF-IR activation of AKT requires estrogen receptor α (ERα) with which IGF-1R physically associates. The ER blocker ICI 182,780 increases the concentration of des-(1–3)IGF-I necessary to activate this cascade, whereas estrogen inhibits both basal AKT activity and its activation by des-(1–3)IGF-I. These data suggest an initial cascade of strain-related events in osteoblasts in which strain activates IGF-IR, in association with ERα, so initiating phosphatidylinositol 3-kinase/AKT-dependent activation of β-catenin and altered lymphoid-enhancing factor/T cell factor transcription. This cascade requires prostanoid/nitric oxide production and is independent of Wnt/LRP5.

The strains that bones experience during everyday mechanical loading are generally accepted as providing the functional stimulus by which they adjust their mass and architecture to withstand these loads without gross fracture or undue accumulation of microdamage. The cells responsible for the initial transduction of strain-related information are the osteoblasts and osteocytes that are in close physical association with the tissue subjected to strain. A number of signaling pathways are activated in the first few minutes following an episode of strain. These include the following: fluxes in calcium (1–5) and production of PGs[2] (3–5), NO (2, 6–9), and ATP (10–13). These pathways precede secondary strain-related events, which include the activation of β-catenin (14–17), increased IGF signaling (3, 18–21), and the suppression of sclerostin production (17).

Given the number of pathways that are stimulated by mechanical strain, it is likely that adaptive remodeling is a result of an integrated network of pathways that function to control bone mass and structure, rather than one pathway uniquely dedicated to mechano-transduction. A contributor to more than one stage in a number of these post-strain cascades is ERα (22–24). ERα is required for strain-related production of NO (24), as well as strain-related translocation of β-catenin to the nucleus (14). Exposure of bone cells to strain activates ERK1/2 in a manner requiring ERα (25). In turn, ERK1/2 activated by strain results in the phosphorylation of ERα (2) and subsequent activation of estrogen-response elements.

Although the nature of the facilitatory role of ERα in these strain-related processes in bone cells is unclear, its practical significance is likely to be high in the light of the crucial role played by estrogen in the etiology of post-menopausal osteoporosis in women and age-related bone loss in men (23, 26). To establish the scope of ERα in the adaptive responses of bone cells to strain, we therefore investigated its relationship with

* This work was supported by the Wellcome Trust.
⌘ *Author's Choice*—Final version full access.
[1] To whom correspondence should be addressed. Tel.: 44-207-468-5046; Fax: 44-207-468-5204; E-mail: asunters@rvc.ac.uk.

[2] The abbreviations used are: PG, prostaglandin; IGF-IR, insulin-like growth factor I receptor; IGF, insulin-like growth factor; PI3K, phosphatidylinositol 3-kinase; ER, estrogen receptor; NO, nitric oxide; ERK, extracellular signal-regulated kinase; HA, hemagglutinin; ANOVA, analysis of variance; WT, wild type; PBS, phosphate-buffered saline; ERKO, ERα knock-out; TCF, T cell factor; Lef, lymphoid-enhancing factor; E_2, estradiol; LRP, low density lipoprotein receptor.

insulin-like growth factor (IGF), another important mediator of the strain-related responses of bone cells. IGF-I and II both play a significant role in the regulation of bone mass. During fetal and juvenile development, IGF-I production by the liver, acting under the control of growth hormone, is one of the chief determinants of bone growth. Individuals lacking growth hormone, IGF-I, or IGF-I receptor (IGF-IR) exhibit reduced stature (27, 28) and bone mineral density (29). However, in the normal adult, the major functional determinant of bone mass is adaptive (re)modeling controlled by functional loading. This process is associated with local autocrine/paracrine production of IGF (30–34). In osteoblastic cells, ERα is required for activation of IGF signaling (35) as is the case in neuronal cells (36–38). Although these data strongly suggest a role for cross-talk between IGF-I and ERα signaling in the propagation of adaptive bone (re)modeling, the precise molecular mechanism responsible and the downstream targets remain undetermined. One pathway capable of being activated by IGFs that could act as a downstream effector for ERα and IGF interaction in osteoblasts is the phosphatidylinositol 3-kinase/protein-kinase B pathway (PI3K/AKT).

PI3K is activated by numerous receptor tyrosine kinases, including the IGF-I receptor, and is responsible for activating the serine/threonine kinase AKT, which plays a significant role in maintaining proliferation and promoting cell survival (39–41). There is evidence that PI3K/AKT signaling is important in determining bone mass; AKT1 knock-out mice are osteopenic (42), whereas mice lacking the PI3K inhibitor PTEN have elevated levels of active AKT and life-long accumulation of bone mass (43). Removal of functional loading results in inhibition of PI3K and AKT (44). In osteoblast-like cells *in vitro*, AKT can be activated by strain, stretching, and fluid flow (45–47).

AKT is able to phosphorylate and inactivate GSK-3β and so regulate β-catenin activity and subsequent Lef/TCF-mediated transcription in cardiomyocytes and HepG2 cells (48, 49). High doses of glucocorticoids result in inhibition of β-catenin in osteoblasts, a response that is in part dependent on AKT (50). Conversely, mechanical strain regulates the levels of activated β-catenin through its effect on AKT in a mouse calvarial osteoblast cell line (45). In breast cancer and endometrial cells, activated AKT is capable of directly phosphorylating ERα to stimulate transcriptional activity (51–53). Some of the effects of ERα/estrogen can be mediated by the PI3K-AKT pathway (54, 55), and in some situations AKT activation is dependent on the nongenomic action of ERα (52, 56, 57). These findings implicate AKT in interacting with three of the key contributors to the strain response, namely IGF, canonical Wnt signaling via β-catenin, and ERα.

That the activation state of AKT should correlate well with anabolic or catabolic activity of bone should not be surprising because AKT controls these processes in many cell types (39). What is important in the context of mechanically adaptive response of bones is how the activity of AKT is controlled and how AKT targets respond to facilitate the anabolic and catabolic (re)modeling activity, which results in alterations in bone mass and adjustments in bone architecture.

In this study, we report that a single episode of mechanical strain stimulates the activation of β-catenin in the absence of increased Wnt/LRP5/Frizzled receptor signaling. This pathway involves IGF-dependent activation of IGF-IR that stimulates PI3K-mediated activation of AKT. AKT in turn generates inhibitory phosphorylation of GSK-3β resulting in activation of β-catenin and stimulation of Lef/TCF-mediated transcription. This pathway requires NO/PG signaling. Mechanical strain primes ERα via an unidentified mechanism (possibly involving its translocation to the membrane) to interact physically with IGF-IR. This interaction lowers the threshold levels of IGF-I necessary to stimulate IGF-IR activation. The relationship between the deficiency of ERα in patients with osteoporosis and in ERKO mice and their attenuated response to loading may in part be explained by a failure of prevailing IGF levels to activate IGF-1R in the absence of sufficient ERα.

EXPERIMENTAL PROCEDURES

Materials—The super8XTOPFLASH (superTOP) reporter construct containing eight Lef/TCF-binding sites within a pTA-Luc vector driving the expression of firefly luciferase under the control of a minimal TA viral promoter was a kind gift of Prof. Randall T. Moon (Howard Hughes Medical Institute and Department of Pharmacology, University of Washington School of Medicine, Seattle). The OPNpGL3 and mOPNpGL3 luciferase reporter constructs containing the 2.3-kbp fragment rat osteopontin promoter and containing two Lef/TCF-binding sites in the native and mutant form were a gift from Prof. Lukas A. Huber (Biocenter, Division of Cell Biology, Medical University Innsbruck, Austria). The pLNCX1-myr-AKT1 and pLNCX1-myr-AKT2 plasmids expressing hemagglutinin (HA)-tagged AKT1 and -2 fused with a membrane targeting myristoylation domain (58) were a kind gift of Dr. Mark Cleasby (Royal Veterinary College, London, UK). The plasmid pcDNA3.1-Dkk-1 was generated by digestion of pCS2-Dkk1-FLAG with EcoRI and XhoI, followed by ligation of the DKK-1 cDNA-FLAG tag into the EcoRI-XhoI site of pcDNA3.1 (59). ERKO null mutant mice were a gift from Prof. Pierre Chambon (Institut de Génétique et de Biologie Moléculaire et Cellulaire, Illkirch-Cedex, France). The antibody recognizing active β-catenin (8E7) was purchased from Upstate Signaling (Dundee, Scotland, UK). Antibodies recognizing β-catenin (E-5), β-actin (I-19), ERα (MC-20), and lamin B (C-20) were purchased from Santa Cruz Biotechnology (Santa Cruz, CA). The anti-Ser-473 phospho-AKT (4060), total AKT (9272), anti-Ser-9 phospho-GSK-3β antibody (9336), anti-GSK-3β (9315), and anti-phospho- and total IGF-IR (3021 and 3027) primary antibodies were obtained from Cell Signaling Technologies (Hitchin, UK). The mouse monoclonal antibody recognizing ERα (SRA1000) was purchased from Cambridge Bioscience (Cambridge, UK). For Western blotting, the primary antibodies were detected using horseradish peroxidase-linked anti-mouse, -goat, or -rabbit conjugates as appropriate (Dako, Ely, UK). For immunocytochemistry, Alexa-conjugated goat anti-mouse IgG secondary antibody was used (Molecular Probes, Edinburgh, Scotland, UK). The following chemicals were purchased from Tocris (Bristol, UK); API-2, LY294002, NS398, L-NAME, SNAP, and ICI 182,780. API-2, LY294002, and NS398 were dissolved in DMSO, and L-NAME and SNAP were dissolved in water immediately before use, and ICI 182,780 was dissolved in ethanol. The IGF-IR inhibitor H1356 was purchased from

Bachem (St. Helens, UK) and dissolved in PBS. The inhibitors AH6809 and AH23848 were obtained from Sigma and dissolved in DMSO. Des-(1–3) receptor grade IGF-1 was obtained from Novozymes-Gropep (Adelaide, Australia) and dissolved in 10 mM HCl and then diluted in PBS containing radioimmunoassay grade bovine serum albumin (0.1 mg/ml).

Cell Culture—The rat osteoblast-like osteosarcoma cell line UMR-106 and primary mouse osteoblasts were maintained in phenol red-free Dulbecco's modified Eagle's medium supplemented with 10% fetal bovine serum, 2 mM glutamine, and 100 units/ml penicillin/streptomycin (complete media), in a humidified incubator in an atmosphere of 5% CO_2 at 37 °C. Primary osteoblast-like cells were prepared from the long bones of 17-week-old female ERKO mice and their wild type (WT) littermates, as detailed previously (3), and cultured as above. Mouse fibroblasts stably transfected with either β-galactosidase or Wnt-I have been described previously (60) and were a kind gift of Dr. Steve Allen (Royal Veterinary College, London). Cells to be subjected to mechanical strain were seeded onto sterile custom-made plastic strips at 10,000 cells/cm^2 (for Western blotting) in a volume of 11 ml of complete media. For reporter assays cells were seeded at 6,000 cells/cm^2. For treatments with ectopic factors (PGs and NO donor IGF-I), cells were seeded at 10,000 cells/cm^2. Cells were washed three times in PBS and cultured in media containing 2% charcoal dextran-stripped fetal calf serum for 2 days before treatment.

Mechanical Straining of Cells—Cells cultured on tissue culture strips were subjected to 600 cycles of four-point bending at a frequency of 1 Hz with a peak strain of 3400 microstrains ($\mu\epsilon$) as described previously (14).

Transient Transfections and Luciferase Assay—UMR-106 cells were transiently transfected with an internal control plasmid pCMV-RL or test plasmid for 16 h using Effectene (Qiagen, Crawley UK) according to the manufacturer's instructions. Following transfection, the cells were washed in PBS, and fresh complete media were added. After treatment, the cells were washed in ice-cold PBS. The cells were then processed, and luciferase activity was determined according to the Dual-Luciferase^{TM} assay system (Promega, Southampton, UK).

Western Blotting—Cells on strips were briefly washed twice in ice-cold PBS and lysed in denaturing lysis buffer (2% SDS, 2 M urea, 8% sucrose, 20 mM sodium β-glycerophosphate, 1 mM NaF, and 5 mM Na_2VO_4) using 100 μl/strip. Genomic DNA was sheared by passage through a Qiashredder column (Qiagen, Crawley, UK) and denatured by boiling for 5 min. Nuclear and cytoplasmic fractionation was performed by a modification of the method described previously (14). Briefly, cells were trypsinized and washed twice in ice-cold PBS and lysed on ice for 15 min in 100 ml of cytoplasmic lysis buffer (10 mM HEPES, pH 7.4, 10 nM KCl, 0.01 mM EDTA, 0.1 mM EGTA, 2 mM dithiothreitol, 5 mM Na_2VO_4, 20 mM sodium β-glycerophosphate, 0.1% Nonidet P-40 and Halt protease inhibitor mixture (Perbio, Chester, UK)). Nuclei were sedimented by centrifugation, and the supernatant containing the cytoplasmic fraction was removed. Urea and SDS were added to a final concentration of 2 M and 2% respectively, and the samples were denatured by boiling for 5 min. The nuclei were then washed in 1 ml of cytoplasmic lysis buffer to remove any contaminating cytoplasm and re-sedimented. The nuclei were then lysed in 100 μl of denaturing lysis buffer as before. Protein concentrations were determined by the BCA assay (Pierce/Perbio, Chester, UK). For Western blotting, 20 μg of protein was size-fractionated using SDS-PAGE and electro-transferred onto Protran nitrocellulose membranes (Schleicher and Schuell). Membranes were blocked for 1 h in 0.2% (w/v) I-block (Topix, Bedford, MA) before being incubated with specific antibodies diluted 1:1000. Primary antibodies were detected using horseradish peroxidase-linked anti-mouse, -goat, or -rabbit conjugates (DAKO, Cambridge, UK) as appropriate and visualized using the enhanced chemiluminescence detection system (GE Healthcare).

Immunoprecipitation—Immunoprecipitation was performed as described previously (61). Briefly, treated cells were lysed in Tween lysis buffer (TLB: 50 mM HEPES, 2.5 mM EGTA, 1 mM EDTA, 150 mM NaCl, 0.1% Tween 20, 1 mM NaF, 1 mM $NaVO_4$, 30 mM β-glycerophosphate, 1 mM dithiothreitol, 100 mg/ml phenylmethylsulfonyl fluoride, and Halt Protease inhibitor mixture (Pierce/Perbio), pH 8.0) with sonication. Protein concentration of the soluble fraction was determined with the BCA protein assay (Pierce/Perbio). 1 mg of cellular extract was precleared with 20 μl of a 50% (v/v) slurry of protein G (GE Healthcare) in a volume of 1 ml of TLB for 30 min at 4 °C and then sedimented by centrifugation. The supernatant was then incubated with 0.5 μg of SRA1000 mouse monoclonal anti-ERα antibody or control mouse IgG for 16 h at 4 °C. Antibodies were immobilized by the addition of 20 μl of a 50% (v/v) slurry of protein G (GE Healthcare) for 30 min at 4 °C. The pellets were washed eight times in 1 ml of TLB before being size-fractionated by SDS-PAGE and Western-blotted.

Immunocytochemistry—After treatment, strips or coverslips were washed in PBS, and the cells were fixed with ice-cold methanol on ice for 10 min followed by two PBS washes. The cells were then permeabilized in 20 mM HEPES, 300 mM sucrose, 50 mM NaCl, 3 mM $MgCl_2$, 0.05% sodium azide, 0.5% Triton X-100 (Surfact-Amps^{TM} X-100, Pierce/Perbio), pH 7.0) for 10 min on ice. Slides were blocked by incubating the slides in "wash buffer" (0.05% sodium azide, 10% fetal calf serum in TBST) for 1 h at room temperature before incubation with primary antibody recognizing active β-catenin (1:100 dilution) overnight at 4 °C. Slides were washed three times for 5 min at room temperature in TBST before incubation with the secondary antibody (Alexa 488-conjugated goat anti-mouse diluted 1:100 (Invitrogen)) for 45 min in the dark at room temperature. Cells were then washed twice in wash buffer. Slides were mounted in Vectorshield containing 4′,6-diamidino-2-phenylindole (Vector Laboratories, Peterborough, UK) before visualization by confocal microscopy using a Leica SP5 confocal microscope with LA5 LF software.

Quantitative Reverse Transcription-PCR—Total RNA was extracted from control and treated cells at specified time points using RNeasy Plus mini kit (Qiagen). Integrity of RNA was verified electrophoretically by ethidium bromide staining and by A_{260}/A_{280} absorption ratio >1.95. One mg of the total RNA from loaded and control tibiae was reverse-transcribed with Superscript II reverse transcriptase (Invitrogen). QuantiTect SYBR Green PCR kit (Qiagen) and Opticon 2 Lightcycler (MJ

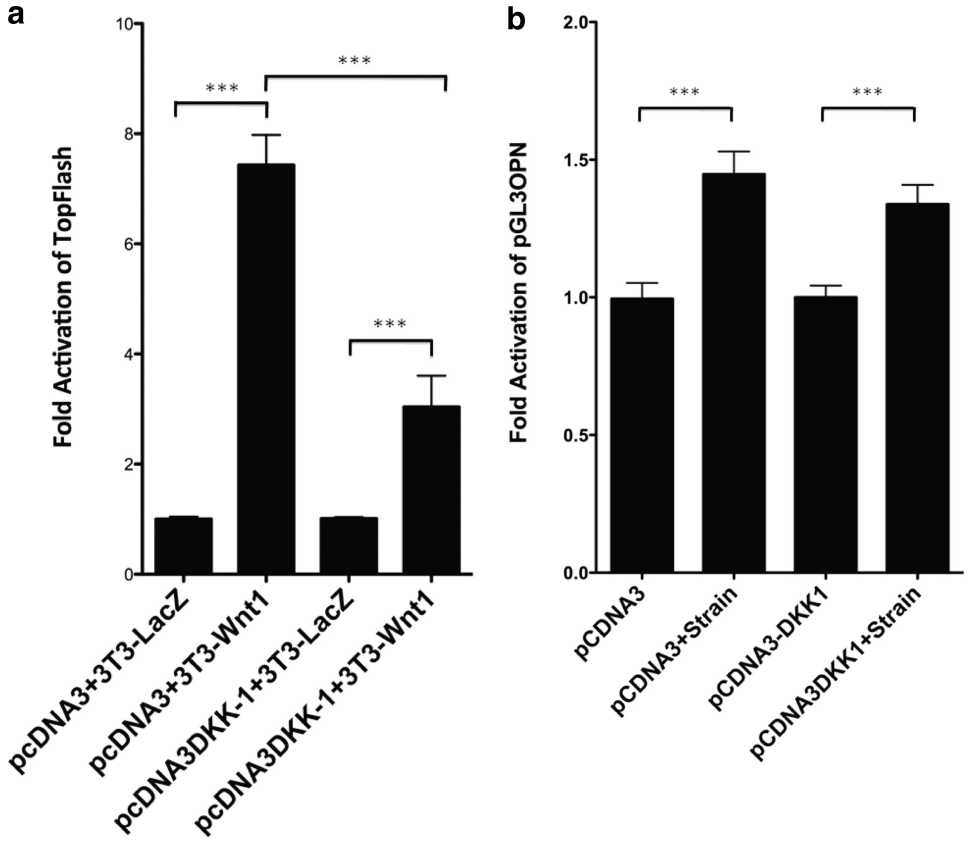

FIGURE 1. **Effect of ectopic expression of Dickkopf 1 (DKK-1) on Lef/TCF signaling initiated by Wnt-1 and mechanical strain.** *a,* UMR-106 cells were transfected with a mixture of 70% pCDNA3 or pCDNA3.1-DKK1, 20% pSuperTOP, and 10% pCMV-RL in 24-well plates. UMR-106 cells were then co-cultured with control 3T3 cells stably transfected with β-galactosidase or 3T3 cells stably transfected with a Wnt-1 expressing plasmid at 300,000 cells per well. Cells were harvested 32 h late, and the relative luciferase activity was determined. Data are represented as corrected luciferase, mean ± S.E., for data pooled from three separate experiments. ***, $p < 0.001$ by one-way ANOVA with Bonferroni post hoc analysis. *b,* UMR-106 cells were transfected with a mixture of 70% pCDNA3 or pCDNA3.1-DKK1, 20% pGL3OPN, and 10% pCMV-RL and subjected to strain by 4-point bending (10 min, 1 Hz, 3400 microstrains, 600 cycles). Cells were harvested 32 h later, and relative luciferase activity was determined. Data are represented as corrected luciferase activity, mean ± S.E., for data pooled from three separate experiments. ***, $p < 0.001$ by one-way ANOVA with Bonferroni post hoc analysis.

Research, Waltham, MA) were used to perform quantitative reverse transcription-PCR. Primers used for the amplification of IGF-I gene were 5′-CTGGATTTCCTTTTGCCTCA and 5′-GCTGGTAAAGGTGAGCAAGC. Primers used for the amplification of β-actin were 5′-CTATGAGCTGCCTGACGGTC and 5′-AGTTTCATGGATGCCACAGG. A standard curve was constructed for IGF-I and the housekeeping gene, and these standards were included in each run. Standards were run in duplicate and samples in triplicate. Samples of unknown concentration were quantified relative to their standard curve. Gene expression levels were normalized to the housekeeping gene β-actin. The PCR conditions used a 15-min initial enzyme activation step followed by 34 cycles of 15 s at 94 °C, 30 s at 60 °C, and 30 s at 72 °C. The final elongation step was 7 min at 72 °C.

Image Analysis—Western blots were analyzed using the ImageJ program, and band volumes were quantitated.

RESULTS

Strain-related Increases in Lef/TCF Activity in Osteoblast-like Cells Do Not Involve the LRP5/Frizzled/Wnt Receptor—We have previously reported that in osteoblast-like cells a single period of dynamic strain is sufficient to increase levels of active β-catenin, stimulating both its entry into the nucleus and elevating Lef/TCF-dependent transcription (14). However, the mechanism by which β-catenin activation occurs is not clear. To determine whether the strain stimulates Lef/TCF activity via increased Wnt signaling through the LRP5/Frizzled/Wnt co-receptor, UMR-106 cells were transiently transfected with the super-TOP Lef/TCF reporter gene as well as pCM-RL and either empty vector DNA (pcDNA3) or the DKK-1 expressing vector pcDNA3.1-DKK1. After 24 h, mouse 3T3 fibroblasts stably transfected with either β-galactosidase or Wnt-1 were added to the transfected UMR-106 cells in co-culture. The relative luciferase activity was determined 32 h later. Fig. 1*a* shows that in empty vector controls, the relative luciferase activity is higher in UMR-106 cells co-cultured with Wnt-1 producing 3T3 cells compared with β-galactosidase-expressing control cells. This demonstrates that UMR-106 cells activate Lef/TCF signaling in response to Wnt. However, in cells ectopically expressing DKK-1, the increase in relative luciferase activity following co-culture with Wnt-1-producing cells was significantly lower than that in empty vector control cells. This indicates that, in this model, ectopic expression of DKK-1 is able to inhibit Lef/TCF activity when stimulated by Wnts. Interestingly, ectopic DKK-1 expression does not reduce the basal relative luciferase activity, suggesting that in this model the normal levels of Wnts (and thus Wnt signaling) may be quite low. To determine whether the increased Lef/TCF activity we have observed to follow exposure to strain is also mediated by Wnt signaling, we performed transient transfection experiments using reporter constructs where luciferase transcription is driven by a fragment of the osteopontin promoter containing two Lef/TCF consensus sites (14). Cells were also co-transfected with either pcDNA3 or pcDNA3-DKK1. The cells were then subjected to a short period of dynamic strain 24 h after which the relative luciferase activity was determined. A modest increase in luciferase was observed following strain (Fig. 1*b*), which, unlike that following addition of Wnt1, was not blocked by the ectopic expression of DKK.

Strain in Osteoblasts Increases Levels of Active AKT, Which Correlates with Inhibition of GSK-3β and Increased Levels of Active β-Catenin—The strain-related increase in β-catenin signaling that we have described previously correlated with the

inhibition of GSK-3β, as determined by increased phosphorylation of Ser-9 (14). Because AKT is a Ser/Thr kinase capable of phosphorylating this site on GSK-3β, we next sought to establish whether this strain-related inhibitory phosphorylation of GSK-3β was mediated by activation of AKT.

UMR-106 osteoblast-like cells were subjected to a single short period of 4-point bending and the expression levels of active (Ser-473 phosphorylated) AKT, inactive GSK-3β (Ser-9 phosphorylated), and active β-catenin measured by Western blotting. The data shown in the representative Western blot (Fig. 2*a*) indicate that although the levels of total AKT protein remain constant, the levels of active AKT become slightly elevated after strain, peaking at 3 h and declining after 4 h. Quantitation of the levels of phosphorylated AKT relative to total AKT was performed using scanning densitometry. This demonstrated statistically significant differences only seen 3 and 4 h after strain. The levels of Ser-9-phosphorylated (inactive) GSK-3β relative to total GSK-3β increased 1 and 2 h following strain, peaked at 3 and 4 h, and declined thereafter. Quantitative densitometry demonstrated that these differences were only statistically significant 3 and 4 h after strain. Similarly, there was a strain-dependent increase in active β-catenin 1 and 2 h following strain, again peaking after 3 and 4 h. Statistical analysis of densitometric scans revealed that these differences were only significant 3 and 4 h following strain. Taken together these data suggest a correlation between the activation of AKT and the increase in inhibitory phosphorylation of GSK-3β, which results in the activation of β-catenin (Fig. 2, *a* and *b*).

Strain-related Activation of β-Catenin Is Mediated by PI3K Activation of AKT—To confirm that AKT is activated in a P13K-dependent manner and that AKT activation is necessary for strain-related activation of β-catenin, UMR-106 cells were pretreated with the PI3K inhibitor LY294002 or the selective AKT inhibitors API-2 (which is a direct inhibitor of AKT activity) or AKT1/2 (which inhibits AKT activation in a pleckstrin homology domain-dependent fashion) for 1 h before being subjected to strain. Lysates were prepared 3 h later (the time point at which strain-induced AKT phosphorylation is statistically significant). Scanning densitometry of replicate Western blots (a representative blot is shown in Fig. 3*a* and quantitative data in Fig. 3*b*) demonstrates that the strain is associated with increased levels of AKT and GSK-3β phosphorylation indicating activation and inhibition, respectively. These changes correlate with increased levels of active β-catenin. However, pretreatment of the cells with LY294002, API-2, or AKT1/2 prevents the strain-related activation of AKT, inhibition of GSK-3β, and the activation of β-catenin. This indicates that strain-related activation of β-catenin is dependent on PI3K activation, phosphatidylinositol 1,4,5-trisphosphate-mediated recruitment of AKT to the membrane via its pleckstrin homology domain (and thus dependent on the presence of phosphatidylinositol 1,4,5-trisphosphate produced by PI3K), and direct kinase activity of AKT.

Strain-related Nuclear Translocation of β-Catenin Requires AKT Activation—In this experiment we sought to establish whether the strain-related nuclear localization of β-catenin, which we had previously identified in the ROS 17/2.8 osteoblastic cell line, also occurred in UMR-106 cells and, if so, whether

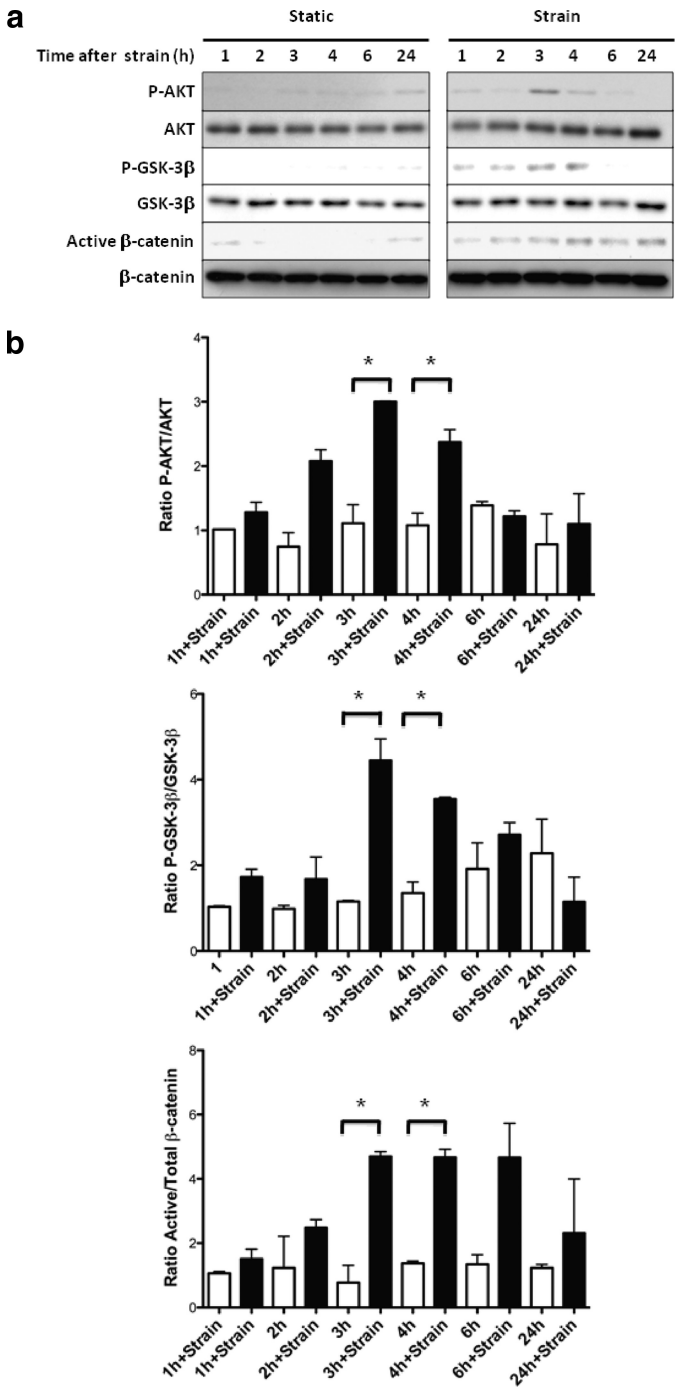

FIGURE 2. **Mechanical strain induces activation of AKT and β-catenin.** *a,* whole cell lysates were prepared from UMR-106 osteoblast-like cells subjected to strain by 4-point bending (10 min, 1 Hz, 3400 microstrains,, 600 cycles) 1- 4, 6, and 24 h following strain. The levels of total and phospho-AKT and GSK-3β as well as total and active β-catenin were analyzed by Western blotting. A Western blot for actin is also shown as a control for equal loading. *b,* scanning densitometry was performed on Western blots from three independent experiments, and the results are represented as fraction of the control. Values shown are mean ± S.E. *, $p < 0.05$ by unpaired two-tailed *t* test.

it was dependent upon AKT activity. To achieve this, we subjected UMR-106 cells to strain following a 1-h pretreatment with vehicle (DMSO) or 20 μM API-2. After 3 h, the cells were fixed in methanol, stained with an antibody recognizing active β-catenin (green), counterstained with the fluorescent DNA-binding dye 4′,6-diamidino-2-phenylindole (to reveal the

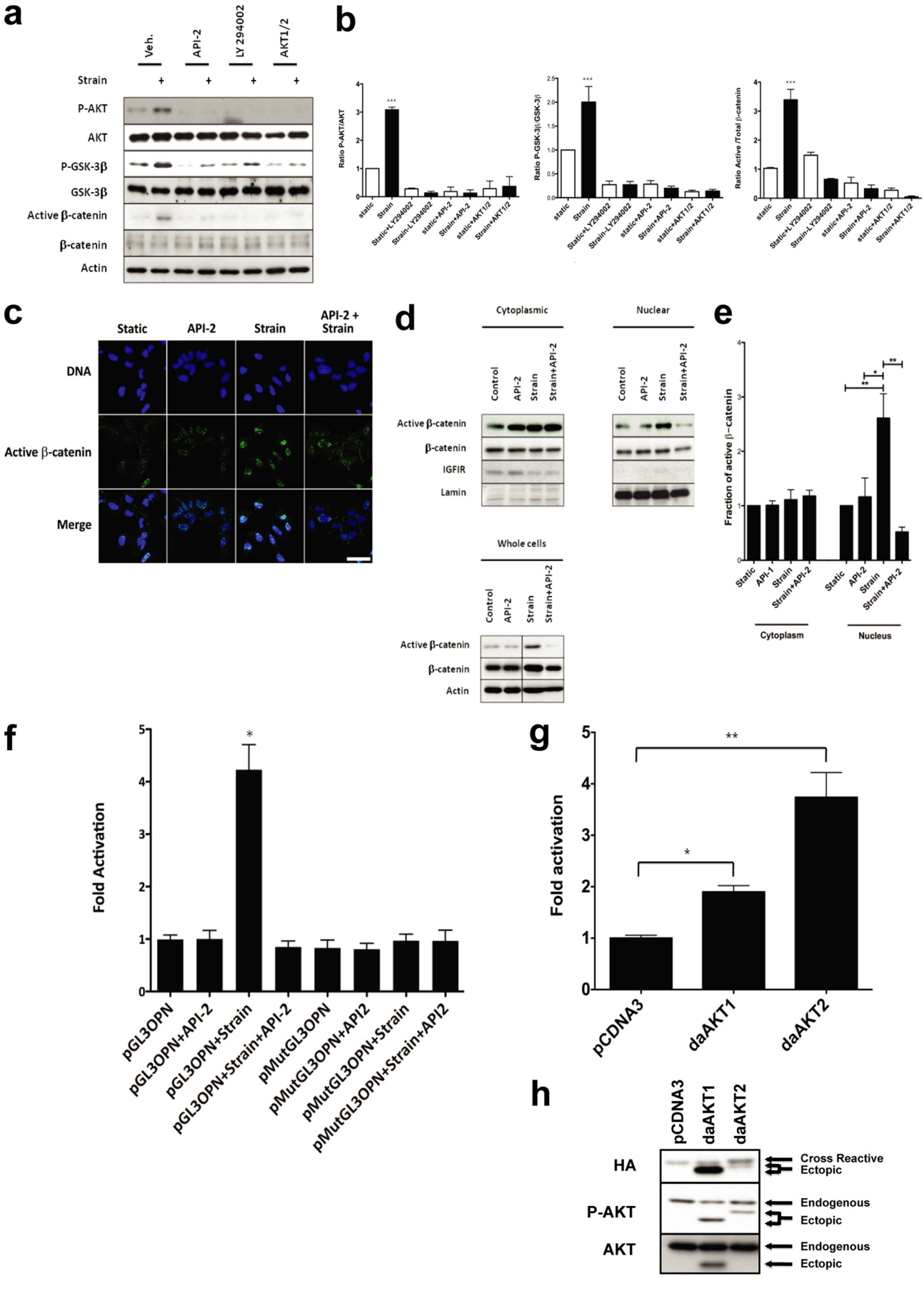
a
Veh.
API-2
LY 294002
AKT1/2
Strain
P-AKT
AKT
P-GSK-3β
GSK-3β
Active β-catenin
β-catenin
Actin
b
Ratio P-AKT/AKT
Ratio P-GSK-3β/ GSK-3β
Ratio Active /Total β-catenin
static
Strain
Static+LY294002
Strain+LY294002
static+API-2
Strain+API-2
static+AKT1/2
Strain+AKT1/2
c
Static
API-2
Strain
API-2 + Strain
DNA
Active β-catenin
Merge
d
Cytoplasmic
Nuclear
Control
API-2
Strain
Strain+API-2
Active β-catenin
β-catenin
IGFIR
Lamin
Whole cells
Actin
e
Fraction of active β-catenin
Static
API-1
API-2
Strain
Strain+API-2
Cytoplasm
Nucleus
f
Fold Activation
pGL3OPN
pGL3OPN+API-2
pGL3OPN+Strain
pGL3OPN+Strain+API-2
pMutGL3OPN
pMutGL3OPN+API2
pMutGL3OPN+Strain
pMutGL3OPN+Strain+API2
g
Fold activation
pCDNA3
daAKT1
daAKT2
h
pCDNA3
daAKT1
daAKT2
HA
P-AKT
AKT
Cross Reactive
Ectopic
Endogenous
Ectopic
Endogenous
Ectopic

nucleus in blue), and analyzed by confocal microscopy. In vehicle-treated static control cells, β-catenin is clearly visible in the nucleus, as determined by co-localization with 4′,6-diamidino-2-phenylindole (Fig. 3*c*). Pretreatment of the cells with API-2 results in a reduction in the amount of active β-catenin staining and nuclear localization. In cells that had been subjected to strain, there is an obvious increase in the amount of staining for active β-catenin. This correlates with our previous Western blot analysis (14). The majority of this staining is associated with the nuclei. Pretreatment of the cells with 20 μM API-2 before strain reduces both the increase in β-catenin staining and its nuclear localization. Indeed, in this situation the majority of active β-catenin is in the cytoplasm, concentrated in the perinuclear area.

To confirm these immunocytochemical results, we performed cellular fractionation on cells pretreated with vehicle and API-2 for 1 h before being subjected to strain. After 3 h, nuclei and cytoplasm were separated, and denatured protein extracts were prepared. The levels of active and total β-catenin were then measured by Western blotting. In the vehicle and API-2-treated cells, active β-catenin is readily detectable in both the cytoplasm and nucleus as well as in whole cell extracts (Fig. 3*d*). In the extracts from strained cells, there is a statistically significant increase in the levels of active β-catenin in the nucleus but not the cytoplasm (Fig. 3*d*). The increase in the levels of nuclear β-catenin in response to strain is statistically significantly inhibited by pretreatment with API-2 (Fig. 3, *d* and *e*) and is similar to that seen in whole cell extracts. The levels of total β-catenin remain similar in both nuclear and cytoplasmic extracts, irrespective of treatment. Western blots performed with antibodies recognizing IGF-IR (cytoplasm) and lamin (nucleus) were used as loading controls, demonstrating that there was no cross-contamination of nuclear extract with cytoplasm and vice versa.

That mechanical strain increases the levels of active β-catenin in the nucleus, but has no effect on that in the cytoplasm, indicates an overall increase in active β-catenin levels in these UMR-106 cells following strain. This agrees with the data shown in Fig. 3, *a* and *b*. The absence of any increase in β-catenin in the cytoplasm suggests rapid translocation to the nucleus. These findings also show that β-catenin molecules within the nucleus can be detected with antibodies specific to both total and active β-catenin.

The contrast between the results obtained by immunocytochemistry and subcellular fractionation observed here is in agreement with our previous report (14). The reasons for the differences between immunocytochemistry and subcellular fractionation are unclear but might represent the presence of active β-catenin in higher order complexes in the cytoplasm, which sterically hinder the binding of antibodies during immunocytochemistry but which are denatured in our lysis buffers rendering them detectable. This seems likely because we have observed that when extracts from LiCl-treated cells are prepared using nondenaturing buffers, we are unable to detect the increase in active β-catenin by Western blotting but are able to do so when using denaturing lysis buffers (data not shown). These data demonstrate that repression of AKT by selective pharmacological inhibitors of PI3K or AKT is capable of blocking the activation and nuclear localization of β-catenin resulting from a single exposure to strain, suggesting that in the immediate period following strain it is AKT activity, and not the consequences of engagement of the Lrp5/6-Frizzled-Wnt receptor complex with the Wnt ligand, that is responsible for the activation of β-catenin. This is consistent with the data shown here in Fig. 1 and described in a recent report by Case *et al.* (45).

Strain-related Lef/TCF-dependent Transcription Is Prevented by Inhibition of AKT—The ultimate arbiter of β-catenin function is modulated transcription of Lef/TCF-responsive genes. We therefore sought to determine whether strain-related regulation of Lef/TCF signaling was also dependent on AKT activation. To this end, we performed transient transfection experiments using reporter constructs where luciferase transcription is driven by a fragment of the osteopontin promoter containing two Lef/TCF consensus sites (wild type), as well as a construct in which these sites were mutated.

The results of these experiments (Fig. 3*f*) show that strain leads to a statistically significant increase in luciferase activity in the cells transfected with the reporter construct containing the wild type Lef/TCF sequence but not in those transfected with

FIGURE 3. **Effect of mechanical strain on the activation and nuclear localization of β-catenin and on Lef/TCF transcription is dependent on AKT.** *a*, whole cell lysates prepared from UMR-106 cells were pretreated with vehicle (*Veh.*) (DMSO), the PI3K inhibitor LY294002, or the selective AKT inhibitors API-2 and AKT1/2 for 30 min prior to being subjected to strain. The levels of total and phospho-AKT and GSK-3β as well as total and active β-catenin were analyzed by Western blotting. A Western blot for actin is also shown as a control for equal loading. *b,* scanning densitometry was performed on Western blots from three independent experiments and the results represented as fraction of the control. Values shown are mean ± S.E. *c,* UMR-106 cells were pretreated with API-2 for 1 h prior to being subjected to strain and then cultured for 3 h before being fixed in ice-cold methanol. The subcellular distribution of active β-catenin was determined by immunostaining (*green*), and the nuclei were counterstained with 4′,6-diamidino-2-phenylindole (*blue*) before analysis by confocal microscopy. *Scale bar,* 50 μm. *d,* UMR-106 cells were pretreated with API-2 and strained as before, and nuclear and cytoplasmic protein fractions were extracted. The expression of active and total β-catenin was then analyzed by Western blotting. Also shown is the expression of IGF-IR and lamin-B as loading controls for each fraction to demonstrate the purity of each fraction, as well as a Western blot performed on denatured whole cell lysate. *e,* scanning densitometry was performed on Western blots from three independent experiments, and the results are represented as fraction of the control. Values shown are mean ± S.E., *, $p < 0.05$, analyzed by two-way ANOVA with Bonferroni post hoc analysis. *f,* cells were transiently transfected with pGL3OPN containing a fragment of the osteopontin promoter driving the expression of firefly luciferase that contains two Lef/TCF consensus binding sites (WT) or pMUTPGL3OPN in which the two Lef/TCF sites were mutated, as well as a control RL-CMV *Renilla* plasmid that constitutively expresses *Renilla* luciferase. Cells were subjected to mechanical strain and harvested 48 h later. Firefly activity was measured and normalized to that of *Renilla*. The data shown represent the average ± S.E. of three independent experiments; each plasmid is normalized to the mean of the static control. *, $p < 0.05$ analyzed by two-way ANOVA with Bonferroni post hoc analysis. *g*, UMR-106 cells were transiently transfected with super8XTOPFLASH (superTOP) as well as either control DNA (pCDNA3), pLNCX1-myr-AKT1, or the pLNCX1-myr-AKT2 that expressed constitutively active AKT1 and -2, respectively. Cells were harvested 48 h later, and firefly luciferase activity was measured. The data shown represents the mean ± S.E. of three independent experiments, each normalized to the value of the control DNA, *, $p < 0.05$ by one-way ANOVA with Bonferroni post hoc analysis. *h,* UMR-106 cells were transiently transfected with control DNA (pCDNA3), pLNCX1-myr-AKT1, or the pLNCX1-myr-AKT2 that express constitutively active AKT1 and -2, respectively. Whole cell lysates were prepared after 48 h, and the expression levels of the HA tag present in the ectopic construct as well as phospho-and total AKT were determined by Western blotting.

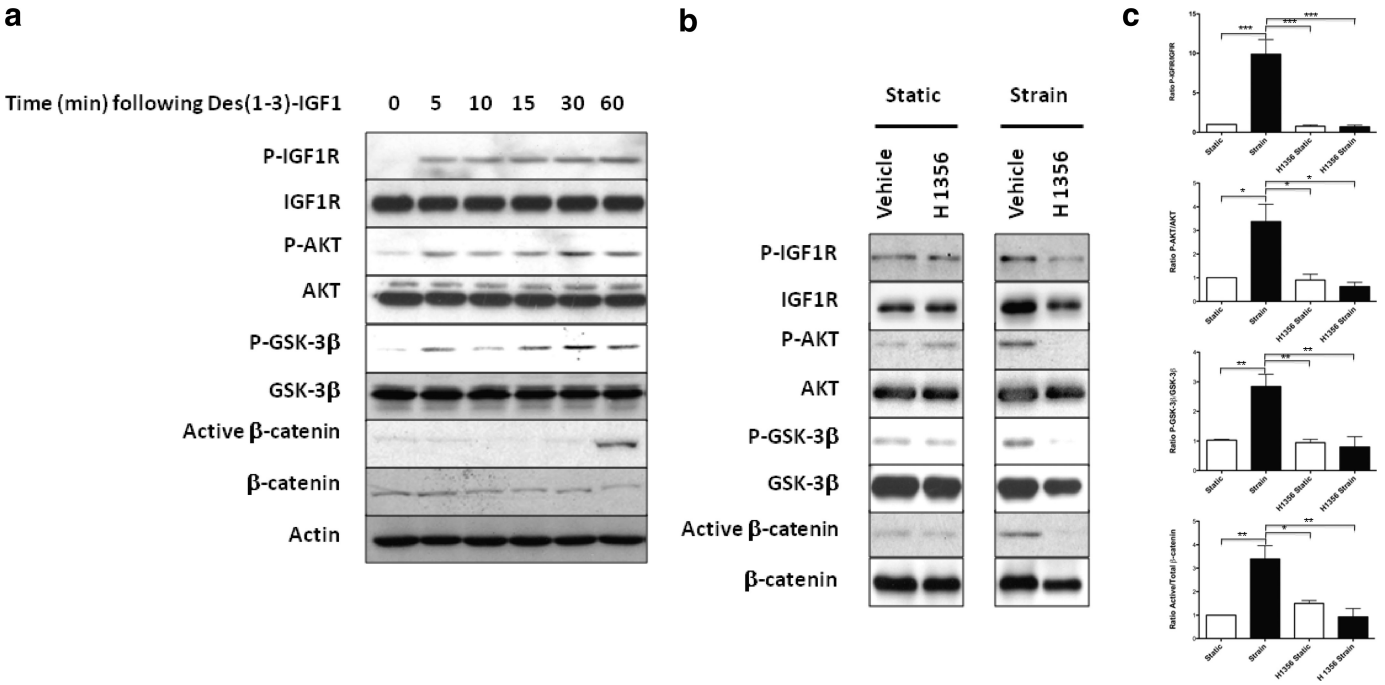

FIGURE 4. **Activation of β-catenin via AKT during the strain response is dependent on IGF.** *a,* whole cell lysates prepared from UMR-106 cells were treated with 50 ng/ml des-(1–3)IGF1 for 5, 10, 15, 30, and 60 min. The levels of total and phospho-AKT and GSK-3β as well as total and active β-catenin were analyzed by Western blotting. A Western blot for actin is also shown as a control for equal loading. *b,* UMR-106 cells were pretreated with vehicle (PBS) or the antagonist H1356 for 30 min prior to being subjected to mechanical strain. Cells were harvested 3 h post strain, and the levels of total and phospho-AKT and GSK-3β as well as total and active β-catenin were analyzed by Western blotting. A Western blot for actin is also shown as a control for equal loading. *c,* scanning densitometry was performed on Western blots from three independent experiments, and the results are represented as fraction of the control. Values shown are mean ± S.E. ***, $p < 0.001$, by one-way ANOVA with Bonferroni post hoc analysis.

constructs in which the Lef/TCF site is mutated. This indicates that the observed increase in luciferase activity following strain is specifically mediated by Lef/TCF. Pretreatment of the cells with API-2 has no effect on the luciferase levels in control cultures transfected with either mutant or wild type constructs, but it completely abrogates the strain-induced increase in luciferase activity in cells transfected with the wild type plasmid. This indicates that strain-related, β-catenin-mediated stimulation of Lef/TCF transcriptional activity is AKT-dependent.

Lef/TCF-dependent Transcription Can Be Driven by AKT Activity—The previous data all demonstrate that AKT inhibition blocks strain-related β-catenin activity. We therefore sought to determine whether the converse was also true, *i.e.* that increased levels of active AKT would stimulate Lef/TCF transcription. To do this, UMR-106 cells were transiently transfected with the superTOP Lef/TCF reporter gene as well as either empty vector DNA (pcDNA3) or constitutively active forms of AKT1 and -2 (pLNCX1-myr-HA-AKT1 and pLNCX1-myr-HA-AKT2). The data shown in Fig. 3*g* demonstrate that transfection of dominant active AKT1 or AKT2 results in a significant increase in luciferase activity relative to the empty vector control. This suggests that AKT activity influences β-catenin-mediated regulation of transcription, which is a critical component of early responses of osteoblasts to strain. To confirm the ectopic expression of AKT1 and AKT2, Western blotting was performed using whole cell extracts of transfected cells. The data from Fig. 3*h* demonstrate expression of the HA tag from both AKT expression vectors but not the empty vector control. A cross-reactive band is detected by the anti-HA antibody in all of the extracts and is indicated in Fig. 3*h*. The use of an antibody that reacts with AKT phosphorylated at Ser-473 detected bands corresponding to endogenous phosphorylated AKT in all extracts and smaller bands in the AKT1- and -2-transfected extracts. These exhibited the same molecular size as the unique bands detected by the anti-HA antibody, which correspond to ectopic AKT. The use of a pan-AKT antibody revealed endogenous bands in all extracts, but it only reacted with the ectopic AKT1 and not AKT2. The reason for this is unclear but may be because the antibody recognizes the C terminus of AKT1, -2, and -3 and that this epitope on AKT2 may have been modified by the cloning procedure.

Taken together, the experiments described suggest a sequence of events in which strain stimulates PI3K-dependent phosphorylation of AKT which in turn leads to inhibition of GSK-3β, thereby activating β-catenin, which translocates to the nucleus where it influences Lef/TCF-dependent transcription.

Strain-related Activation of AKT Requires the IGF-I Receptor—In other situations, one of the major regulators of AKT activity is IGF acting through its receptor, IGF-1R. We have previously demonstrated that IGF production and signaling is required for proliferative response of osteoblasts to strain (3). We therefore sought to establish the role of IGF signaling in regulating the strain-related activation of these cells of the AKT/GSK-3β/β-catenin axis. To do this, we first determined in UMR-106 cells the extent to which activation of IGF-IR by exogenous IGF would mimic the cascade of strain-related events involving activation of AKT, inhibition and activation of GSK-3β, and activation of β-catenin. Fig. 4*a* shows the results of addition of 50 ng/ml des-(1–3)IGF-I (which is not subject to regulation by IGF-binding proteins) to UMR-106 cells cultured in the

absence of serum for 48 h to maximize the effect of des-(1–2)IGFI. Western blotting was used to measure the phosphorylation of IGF-IR, as well as AKT, GSK-3β, and the activation of β-catenin. These data show that addition of des-(1–3)IGF-I stimulates phosphorylation of AKT and GSK-3β within 5 min. Activation of β-catenin was complete after 1 h. This lag between IGF addition and β-catenin activation is not surprising, because a number of steps are required, including either de-phosphorylation of β-catenin and/or the *de novo* synthesis of hypophosphorylated β-catenin to replace that targeted for proteolysis by GSK-3β phosphorylation.

Having demonstrated that addition of IGF-I is capable of mimicking the effects of strain on the AKT/GSK-3β/β-catenin axis, we next sought to identify whether activation of this pathway was a component of the strain-related response. We therefore pretreated UMR-106 cells with 20 μg/ml of the IGF-IR antagonist H1356 for 1 h before subjecting them to strain. Their response in terms of the activation of IGF-IR and AKT, as well as the inhibition and activation of GSK-3β and β-catenin, was analyzed by Western blotting. The data shown in Fig. 4, *b* and *c*, illustrate that strain-induced activation of IGF-IR/AKT/GSK-3β/β-catenin is inhibited by H1356, indicating that strain-induced activation of this pathway is dependent on involvement of IGF-IR. This is consistent with osteoblasts either releasing IGFs in response to strain or increasing their sensitivity to existing levels of IGF.

Cyclooxygenase 2 (COX-2), NO, and PGs Are Required for Strain-related Activation of AKT, but NO and PG Are Unable to Activate AKT Individually—Although the data presented here clearly suggest that exposure of osteoblastic bone cells to mechanical strain leads to the activation of AKT in an IGF-IR-dependent fashion, the mechanism of IGF-1R involvement is unclear. The early responses that occur when bone cells are subjected to mechanical strain include the release of PGs (3, 13, 62) and NO (2, 6–9), which have been demonstrated to be responsible for the release of IGF-I by osteoblasts (3), which would then potentially be able to activate AKT.

To investigate whether it was newly produced IGF that was responsible for increased IGF-1R activity, we treated UMR-106 cells cultured in 2% charcoal dextran-treated fetal calf serum with 5 mM of the NO donor SNAP, as well as both 1 μM prostaglandins E_2 and I_2, respectively, for 15 min and 2 and 6 h. A parallel treatment was also performed with 50 ng/ml des-(1–3)IGF-I. Western blots were undertaken on whole cell extracts, and the levels of active AKT and β-catenin and inactive GSK-3β were measured as described previously. The data from Fig. 5*a* demonstrate that unlike des-(1–3)IGF-I, none of these treatments activated AKT. Although PGE_2 increased activation of β-catenin, reaching a maximum 6 h after treatment, this did not correlate with phosphorylation/activation of AKT or result in the activation of β-catenin to the extent of des-(1–3)IGF-I. Although des-(1–3)IGF-I was capable of activating AKT/GSK-3β/β-catenin cascade, the activation of β-catenin occurred 1 h sooner than that observed in Fig. 4*a*, an observation we attribute to the fact that the experiment shown in Fig. 5*a* was performed in a higher concentration of fetal calf serum, which increases basal activation of this pathway. Although direct stimulation of NO and PG signaling was not capable of stimulating AKT activity, it has been shown that inhibition of these pathways can block IGF-I transcription, suggesting that they may be responsible for maintaining basal levels of IGF-I pro-

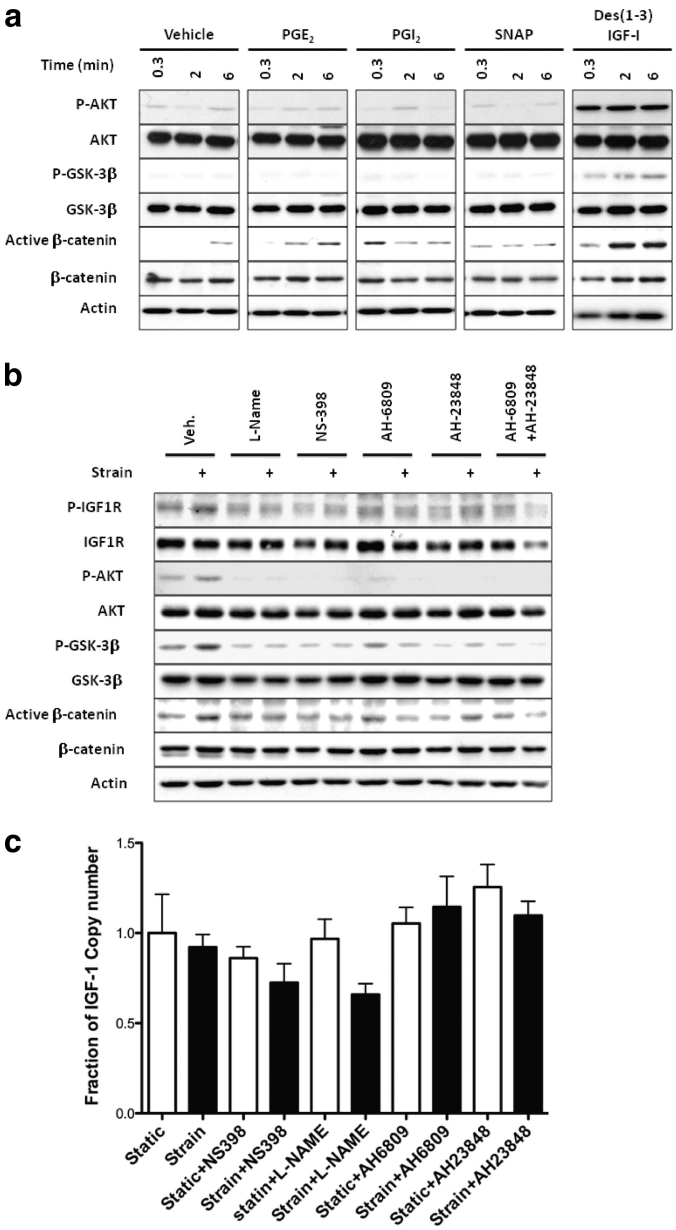

FIGURE 5. **IGF-IR-mediated AKT activation of β-catenin is dependent on basal PG signaling and NO synthesis during the response to mechanical strain.** *a,* whole cell lysates were prepared from UMR-106 cells treated with PGE_2, PGI_2, the NO donor SNAP or des-(1–3)IGF-I for 30 min and 2 and 6 h. Levels of total and phospho-AKT and GSK-3β as well as total and active β-catenin were analyzed by Western blotting. A Western blot for actin is also shown as a control for equal loading. *b,* UMR-106 cells were pretreated with vehicle (*Veh.*) (DMSO), the NO synthase inhibitor L-NAME, the COX-2-selective inhibitor NS398, and the PG receptor antagonists AH6809 and AH-23848 either alone or in combination for 30 min prior to being subjected to strain. Whole cell lysates were prepared 3 h after strain, and the levels of total and phospho-IGF-IR, AKT, and GSK-3β as well as total and active β-catenin were analyzed by Western blotting. A Western blot for actin is also shown as a control for equal loading. *c,* UMR-106 cells were pretreated with vehicle (DMSO), the NO synthase inhibitor L-NAME, the COX-2-selective inhibitor NS398, and the PG receptor antagonists AH6809 and AH-23848 for 30 min prior to being subjected to mechanical strain. Total RNA was extracted from the cells 3 h after strain, and the expression of IGF-I was determined by quantitative real time reverse transcription PCR. Data are expressed as mean ± S.E. ***, $p < 0.001$, by one-way ANOVA with Bonferroni post hoc analysis.

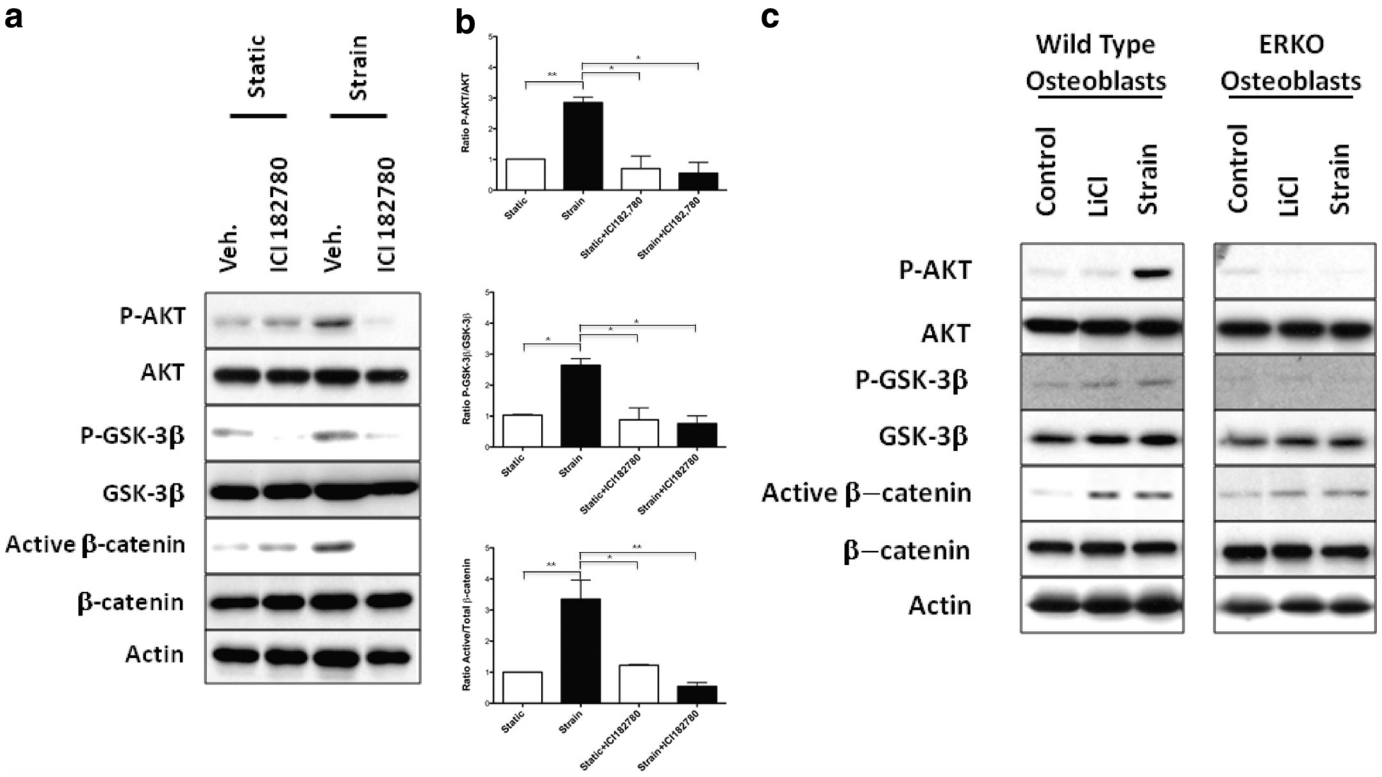

FIGURE 6. **Activation of β-catenin via AKT during the strain response is dependent on the presence of ERα.** *a,* whole cell lysates prepared from UMR-106 cells pretreated with vehicle (*Veh.*) (ethanol) or the pure anti-estrogen ICI 182,780 for 16 h prior to being subjected to strain. Levels of total and phospho-AKT and GSK3-β, as well as total and active β-catenin, were analyzed by Western blotting. A Western blot for actin is also shown as a control for equal loading. *b,* scanning densitometry was performed on Western blots from three independent experiments, and the results are represented as fraction of the control. Values shown are mean ± S.E. *, $p < 0.05$; **, $p < 0.01$ by one-way ANOVA with Bonferroni post hoc analysis. *c,* whole cell lysates were prepared from primary osteoblasts isolated from the long bones of ERKO mice and wild type littermate controls 3 h after being subjected to mechanical strain or treatment with 10 mM LiCl. The levels of total and phospho-AKT and GSK3-β as well as total and active β-catenin were analyzed by Western blotting. A Western blot for actin is also shown as a control for equal loading.

duction. To determine whether this was the case, cells were treated with pharmacological inhibitors of PG production and function prior to their exposure to strain. The data shown in Fig. 5*b* demonstrate that inhibition of NO production by 1 mM L-NAME, COX-2 activity by 3 μM NS398, PG receptor function by 3 μM AH6809 (receptors 1 and 2), or 3 μM AH23848 (receptor 4) all inhibit not only the basal activity of the AKT-GSK-3β/β-catenin pathway but also its activation by strain.

To determine whether the NO/nitric-oxide synthase/COX-2/PG pathways are responsible for changes in IGF-I RNA levels, UMR-106 cells were pretreated with L-NAME, NS398, AH6809, or AH23848 for 1 h before being subjected to mechanical strain. Three hours after the application of strain, RNA was extracted from the cells, and the steady state levels of IGF-1 was measured using quantitative reverse transcription-PCR. Fig. 5*c* demonstrates that these treatments have no effects, whether in control or strained cells, on IGF-I RNA levels. Taken together, these data suggest that in UMR-106 cells the strain-responsive NO and PG pathways are not capable of separately stimulating AKT directly. However, strain-related changes in their combined action, most likely in concert with other strain related pathways, can modify IGF signaling at the level of IGF-1R without involving increased transcription of IGF. Modification of IGF-1R sensitivity to ambient IGF may be an important component of the early stages of the response of osteoblasts to strain.

Strain-related Activation of AKT Requires ERα—We have previously reported that both β-catenin and IGF-I signaling are attenuated in osteoblasts isolated from ERKO mice or osteoblasts treated with the selective ER modulator ICI 182,780. We therefore wished to determine whether this ERα dependence was a feature of strain-related activation of the IGF-IR/AKT/GSK-3β/β-catenin axis. UMR-106 cells were pretreated with 100 nM ICI 182,780 for 16 h before subjecting the cells to strain. The representative blot shown in Fig. 6*a* shows strain-related increases in phospho-AKT, phospho-GSK-3β, and active β-catenin. All of these were abrogated by pretreatment with ICI 182,780 (Fig. 6, *a* and *b*).

To confirm this observation, primary cortical osteoblasts isolated from the long bones of ERKO mice and their wild type C57Bl6 (WT) littermates were subjected to treatment with either 10 mM LiCl, which inactivates GSK-3β, or strain. In the primary osteoblasts from WT mice, both LiCl and strain result in a small increase in phospho-GSK-3β and a larger increase in the levels of active β-catenin. Strain, but not LiCl, results in an increase in the expression of phospho-AKT. In the osteoblasts isolated from ERKO mice, the bands from the actin loading control appeared to be less intense than in the wild type mice, whereas the levels of total AKT and GSK-3β were similar. As in the WT, LiCl treatment was not associated with any increase in phospho-AKT. However, in contrast to the cells from WT mice, those from ERKO mice showed a complete lack of strain-

related AKT phosphorylation. Interestingly, in ERKO osteoblasts there was a slight increase in phospho-GSK-3β and β-catenin activation following strain.

These data demonstrate two important findings as follows: i) that strain-related increase in AKT activity, together with its associated inactivation of GSK-3β and increase in the levels of active β-catenin, occurs in primary cultures of long bone derived osteoblasts as well as in the UMR-106 cell line, and, ii) that in primary osteoblasts, as well as in cells from osteoblastic cell lines, strain-related IGF-IR/AKT/GSK-3β/β-catenin signaling is modified by ERα.

ERα Sensitizes Osteoblasts to Ambient IGF-I—Because strain-related activation of AKT appears to be dependent on both IGF and ERα signaling, we sought to determine whether this could be explained by the previously reported requirement for ERα in IGF-IR signaling (63). To explore this, UMR-106 cells were treated with either vehicle or ICI 182,780 for 16 h to depress ERα protein levels, before being treated with increasing concentrations of des-(1–3)IGF-I. The data shown in Fig. 7*a* demonstrate that in the control cells phosphorylation (activation) of IGF-IR was evident at concentrations of des-(1–3)IGF-I as low as 1 ng/ml. These concentrations correlate with activation of the AKT/GSK-3β/β-catenin pathway. However, in cells treated with ICI 182,780, equivalent activation was only achieved with concentrations of 10 ng/ml IGF-I. This suggests that although the presence of functional ERα is not an absolute requirement for IGF-related activation of AKT, its presence sensitizes IGF-1R to far lower concentrations of des-(1–3)IGF-I. The results of quantitation of three independent experiments are shown in Fig. 7*b* and demonstrate that the inhibition of ERα with ICI 182,780 is capable of attenuating the signaling of IGF-I via the IGF-IR/AKT/GSK-3β/β-catenin pathway.

Des-(1–3) IGF-I Signaling in Osteoblasts Requires E_2-independent ERα Action and Src Kinase Activity—It has been previously demonstrated that ERα is able to interact with IGF-IR to facilitate signaling downstream of IGF-IR in breast cancer cells and neuronal cells. This effect has been shown to be achievable in breast cancer cells by E_2 in the absence of IGF-I and to be dependent on the activity of the Src homology 2 domain activity. Indeed, it has been demonstrated that the recruitment of ERα to the membrane requires the presence of the Shc protein (64, 65). Consequently, we sought to determine whether AKT activation by des-(1–3)IGF-I in UMR-106 osteoblasts could also be mimicked by E_2 and whether it required the presence of Src activity. Consequently, UMR-106 osteoblasts were treated with vehicle, 100 nM E_2, or 1 ng/ml of des-(1–3)IGF-I in the presence of 100 nM ICI 182,780 or the pan-Src inhibitor PP2 (5 nM). The data shown in Fig. 7*c* demonstrate that whereas des-(1–3)IGF-I stimulates AKT phosphorylation, E_2 treatment inhibits the basal activation of AKT rather than activating it. This is in sharp contrast to the situation in breast cancer cells (64, 65). In osteoblastic cells, blockade of ERα with ICI 182,780 depresses basal AKT phosphorylation and inhibits des-(1–3)IGF-I-mediated stimulation of AKT, but it has no further effect on E_2-dependent depression of either basal or des-(1–3)IGF-I-stimulated AKT activity. However, inhibition with PP2 results in a reduction of basal and des-(1–3)IGF-I stimulated AKT phosphorylation, as has been reported in the MCF-7 breast cancer cell model (64, 65).

IGF-IR Physically Associates with ERα in Osteoblasts—To investigate whether the mechanism by which ERα modifies IGF-1R activity involves physical association between ERα and IGF-IR, we performed immunoprecipitation experiments with an antibody recognizing ERα. The data shown in Fig. 7*d* show that ERα and IGF-IR are both present in the input lysates at equivalent levels. Control mouse IgG failed to immunoprecipitate either ERα or IGF-IR. However, Western blotting following immunoprecipitation with an antibody recognizing ERα demonstrated the presence of ERα. Further Western blotting using an antibody recognizing IGF-IR demonstrated that IGF-IR was not present in the immunoprecipitate of the negative control mouse antibody, but it was detectable following immunoprecipitation by the ERα antibody. This demonstrates that ERα and IGF-IR are physically associated in a multiprotein complex. Furthermore, treatment with des-(1–3)IGF-I increases the amount of IGF-IR associated with ERα.

These data support the hypothesis that ERα sensitizes osteoblast-like cells to low doses of IGF-I, possibly via direct physical interaction with IGF-IR. It also highlights a potential difference in the mechanism of IGF-I signaling between the osteoblast like cell line UMR-106 and the MCF-7 breast cancer model insofar as E_2 is inhibitory in the osteoblast model and stimulatory in the breast cancer model. This may reflect our own observations[3] and those of others (66, 67) regarding the differing numbers of estrogen receptors available, *i.e.* a few hundred in osteoblasts and many thousands in breast cancer cells.

DISCUSSION

The data presented here demonstrate that when osteoblast-like cells, either primary cultures of normal mouse long bone-derived osteoblasts or those of the UMR-106 cell line, experience even a single short period of dynamic strain capable of stimulating proliferation *in vitro*, and new bone formation *in vivo*, there is rapid PI3K-mediated activation of AKT, AKT-mediated inhibition of GSK-3β, and increased levels of active nuclear β-catenin. These strain-related changes, which are accompanied by consequent increased Lef/TCF-dependent transcription, do not involve the Wnt/LRP5/Frizzled receptor. The activation of AKT by strain appears to proceed via a mechanism that involves IGF-IR. The ectopic addition of des-(1–3)IGF-I mimics strain-related activation of AKT followed by inhibition of GSK-3β, activation of β-catenin, and its translocation to the nucleus. Of potentially critical importance to the etiology of post-menopausal osteoporosis, IGF-IR-mediated activation of AKT by both strain and IGF involves ERα, which physically associates with IGF-IR. Inhibition of ERα by the selective ER modulator ICI 182,780 increases the concentration of des-(1–3)IGF-I necessary to stimulate IGF-IR-mediated activation of AKT. Interestingly, in this context estradiol inhibits ERα-related activation of IGF-IR because it reduces basal and des-(1–3)IGF-I-dependent phosphorylation of AKT. This suggestion that in osteoblastic cells estradiol competes for ERα

[3] A. Sunters, L. E. Lanyon, and J. S. Price, unpublished data.

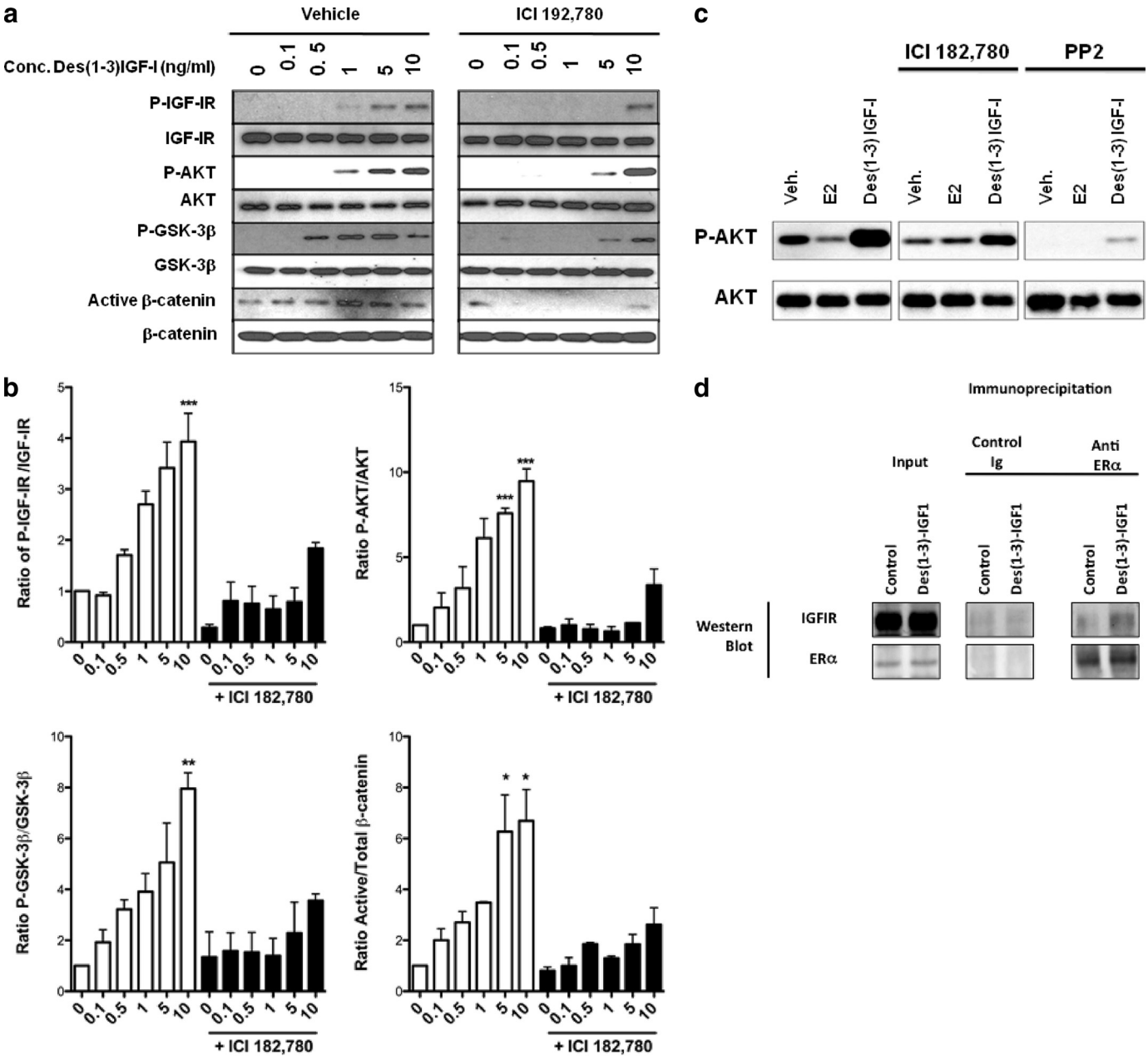

FIGURE 7. **ERα sensitizes UMR-106 osteoblasts to IGF-I in an estrogen-independent fashion requiring Src activity and physically associates with IGF-IR.** *a,* whole cell lysates prepared from UMR-106 cells pretreated with vehicle (ethanol) or ICI 182,780 for 16 h prior to being treated with 1, 0.1, 0.5, 1, 5, or 10 ng/ml IGF1 for 3 h. The levels of total and phospho-AKT and GSK3-β as well as total and active β-catenin were analyzed by Western blotting. *b,* scanning densitometry was performed on Western blots from three independent experiments, and the results are represented as fraction of the control. Values shown are mean ± S.E. ***, $p < 0.001$; **, $p < 0.01$; *, $p < 0.05$ by one-way ANOVA with Bonferroni post hoc analysis. *p* values are only shown in the des-(1–3)IGF-I group when they from the 10 ng/ml des-(1–3)IGF-I + ICI 182,780. *c,* whole cell lysates prepared from UMR-106 cells were pretreated with vehicle (*Veh.*) (ethanol) or ICI 182,780 for 16 h, E_2 (3 h), or the pan-Src inhibitor PP2 (30 min) prior to being treated with 1 ng/ml des-(1–3)IGF1 for 1 h. The levels of total and phospho-AKT were measured by Western blotting. *d,* nondenaturing TLB lysates were prepared from UMR-106 cells treated with 50 ng/ml IGF1 for 3 h. 1 mg of extract was immunoprecipitated with 5 μg of mouse IgG or SR1000 mouse monoclonal antibody recognizing ERα. Immunoprecipitates were analyzed by Western blotting to determine the levels of ERα in the immunoprecipitates and the amount of IGF-IR associated with ERα. Also shown are Western blots for 10 μg of "input" lysate to determine the base-line expression of both ERα and IGF-IR in the lysates.

with IGF1R may have profound consequences for strain-related control of bone (re)modeling when ERα is in short supply.

It has long been recognized that one of the early responses of osteoblasts to strain is increased production of prostaglandins and nitric oxide. We show here that neither of these added exogenously mimics strain-related activation of the AKT/GSK-3β/β-catenin axis. However, blocking the production of NO or PGs, or inhibition of PG receptor signaling, reduces both basal and strain-related activation of IGF-IR and AKT with no change in the levels of IGF-I transcription.

Strain-related Increases in β-Catenin and Lef/TCF Activity in Osteoblast-like Cells Are Dependent on AKT Activation but Do Not Involve the Wnt/LRP5/Frizzled Receptor—We previously reported that a single period of dynamic strain was sufficient to increase levels of active β-catenin in the nucleus of osteoblast-like cells and to elevate Lef/TCF-dependent transcription (14).

Here, we show that the Lrp5/6 inhibitor Dickkopf 1 was able to block Wnt1-dependent, but not strain-dependent, activation of Lef/TCF signaling. This suggests that Lef/TCF activation during the early phase of the strain response is independent of Wnts, thus agreeing with the findings of Case *et al.* (45) who demonstrated that the addition of recombinant Dickkopf 1 was unable to block the increased expression of the Lef/TCF target gene following stretching.

Low AKT activity in osteoblasts correlates broadly with lower bone mass, higher levels of osteoblast apoptosis (42, 44), and attenuated β-catenin signaling (45, 50). Conversely, high AKT activity is associated with higher bone mass (43). This suggests that AKT activity corresponds to the anabolic status of the bone. Given the central role of AKT in regulating cell growth, proliferation, and apoptosis in virtually every cell type in the body, it is not unexpected that AKT should be a central regulator of these parameters in bone.

The importance of AKT in the adaptive response of bones to loading lies first in the mechanism of its specific, strain-related activation and second in the function of its downstream targets. The data we present here, and the observation by others that fluid shear activates AKT, GSK-3β phosphorylation, and nuclear β-catenin translocation in osteoblasts *in vitro* (45–47, 68), support the conclusion that modulation of AKT activity is an early consequence of exposure to mechanical strain.

Our present identification of an early strain-responsive pathway involving AKT-dependent, β-catenin-mediated regulation of Lef/TCF transcription independent of the LRP5/Frizzled/Wnt receptor does not exclude the existence of other Wnt/LRP5/6-dependent strain-related influences on bone (re)modeling. Correlations between bone mass, adaptive responses to strain, and Wnt signaling drawn from LRP gain of function and loss of function phenotypes in both humans and rodents (69–75) suggest that Wnt signaling is involved in bone cell response to mechanical loading. In terms of the temporal kinetics of the strain response, it may be that early activation of β-catenin by AKT and prolonged activation by Wnts maintain an "umbrella" of β-catenin signaling. One consequence of this mixed activation model would be that the repertoire of Lef/TCF target genes activated by β-catenin may be different depending on the mechanism used to activate β-catenin.

Role of IGF/PI3K Signaling in Strain-related Activation of AKT—The data shown here that inhibition of IGF-IR inhibits strain-mediated activation of AKT correlates with our previous observations that IGF signaling is an essential component of the osteoblasts response to strain (18, 35). One of the chief signaling pathways activated by IGF-IR is the PI3K pathway. In osteoblasts, previous data suggest that mechanical perturbations activate AKT via PI3K (68). This contrasts with the recent findings of Case *et al.* (45) who show that strain-related activation of AKT in CIMC-4 calvarial cells occurs independently of PI3K. Possible reasons for this discrepancy include the fact that CIMC-4 calvarial osteoblast-like cells may, like calvaria, have different mechanical responses to strain than long bones and cells derived from them (4). Furthermore, CIMC-4 cells were originally isolated from H-2Kb-tsA58 "imortomouse," which contains a temperature-sensitive SV40 large T antigen (76–79) that is capable of activating AKT independently of PI3K (80–83).

Our hypothesis that IGF signaling may be one of the critical activators of β-catenin via AKT is supported by the observation that in hepatocytes IGF stimulates the AKT/GSK-3β/β-catenin axis (49). These strands of evidence all support the inference that there is a strain-responsive Wnt/LRP5-independent pathway in which β-catenin is activated by PI3K/AKT-mediated GSK-3β suppression. We do not discount the possibility that direct phosphorylation of β-catenin via c-Jun N-terminal kinase (JNK) (84) and AKT (85), both acting under the control of PI3K, could contribute to PI3K-mediated regulation of β-catenin, we only suggest that in osteoblastic cells there is an early strain-responsive pathway where this is not involved.

The relevance of cell type should not be ignored in this context. Although osteoblasts are clearly strain-responsive, osteocytes are considered to be the major mechanosensors within bone. The physical characteristics of the environment of these two cell types differ *in vivo* as may their responses when it is perturbed by loading.

COX-2, NO, and PGs Are Required for Strain-related Activation of AKT, but NO and PG Are Unable Individually to Activate AKT—Early signaling events previously associated with the adaptive response of the bone cells to strain include the production of NO (6, 86) and PGs (4, 5, 62, 87, 88). Administration of inhibitors of either PG or NO production reduces the osteogenic response to loading *in vivo* (89–91). Although we did not observe any direct effect of ectopic addition of NO, PGE_2, or PGI_2 on AKT activation, several reports have documented that this does occur in other cell types (92–97).

Our observation that NO donors or ectopically administered PGs were individually unable to recapitulate strain-related activation of AKT, although antagonists of NO production, COX-2 activity, and PG receptor function prevented AKT activation, suggests that COX-2/PG/nitric-oxide synthase/NO signaling is necessary as a "package" or "multiple key" for the strain-related activation of AKT. However, each individual component, although necessary for the effectiveness of the multiple key, is insufficient individually to stimulate the response. The mechanism for this remains elusive; data that mechanical strain or perturbations to nitric-oxide synthase, NO, COX-2, and PG signaling had no effect on IGF-I transcription within the early stages (up to 3 h) of the strain response suggest that it does not involve transcription. Although we and others have shown that transcription of IGFs does increase with strain and exogenous PGs (3, 8, 18, 91), this occurs after the activation of AKT has peaked (12–24 h).

We therefore envisage a two-phased involvement of IGF-1R in response to strain. In the initial phase, IGF-IR is activated by ambient levels of IGF after having become sensitized to them by a number of different pathways involved in the adaptive response. In the later response IGF-1R is activated again, or its level of activation further increased, by increased ambient IGF following its production in a strain-related, PG-mediated fashion. Under normal circumstances *in vivo*, one episode of strain will be followed by another, the sensitivity of IGF-1R to strain thus being influenced by the previous strain history of the cells.

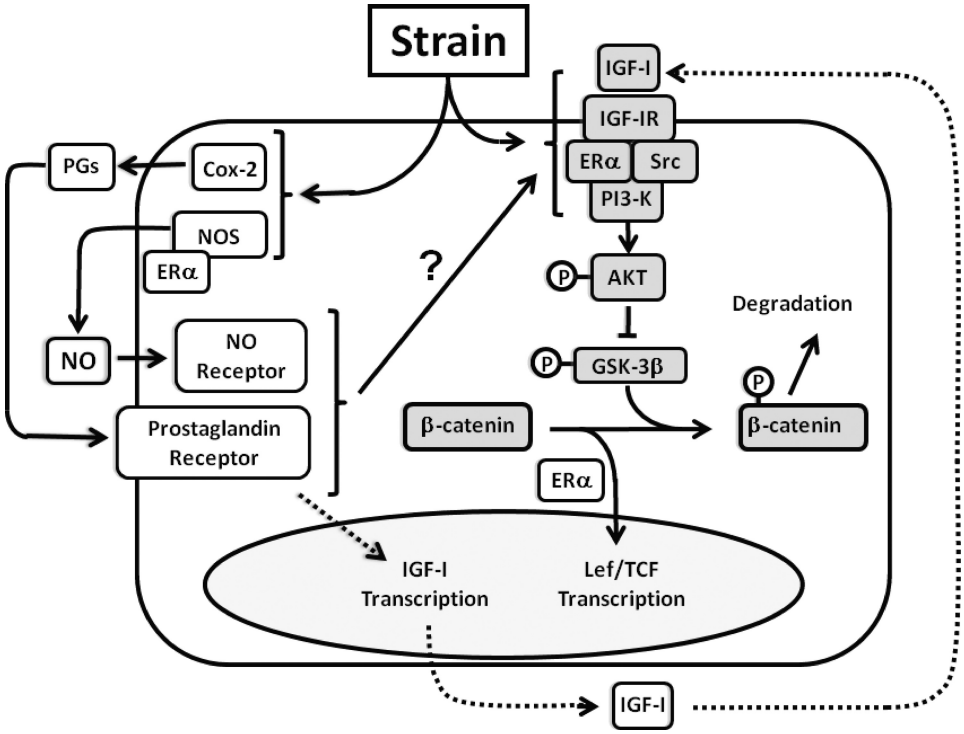

FIGURE 8. **Schematic of the proposed model of β-catenin activation by mechanical strain.** Application of strain results in the increased activation of IGF-IR, an event that is dependent on the presence of ERα, Src activity, and signaling via both NO and prostanoids. IGF-IR then stimulates a PI3K-dependent activation of AKT leading to phosphorylation of GSK-3β thereby inhibiting the ability of GSK-3β to target β-catenin for proteolysis. The increased number of active β-catenin molecules are then free to translocate to the nucleus were they stimulate Lef/TCF-mediated transcription in a Wnt- and LRP5-independent fashion. The later effects of mechanical strain on IGF-I transcription are also illustrated using a *dashed line*. *NOS,* nitric-oxide synthase.

Dependence of IGF Signaling on ERα during the Strain Response of Osteoblasts—We have previously demonstrated that osteoblasts isolated from ERα knock-out mice fail to respond to strain or exogenously applied IGFs (24) and also fail to increase the levels of active β-catenin in the nucleus following strain (14). Here, we show in UMR-106 osteoblast-like cells that ICI 182,780 treatment abrogates strain-dependent β-catenin activation following strain and a reduced activation of β-catenin in ERKO-derived primary osteoblasts, which may reflect a compensatory mechanism in the knock-out cells. Taken together, this evidence suggests that ERα is an important component in the strain-dependent pathway responsible for β-catenin activation. These could be explained by our present finding that IGF-I activates β-catenin via AKT and that this process requires the presence of ERα. There is evidence of ERα and PI3K/AKT interacting to determine the strength of IGF-I signaling in breast cancer and the uterus (57, 98). The data we show here demonstrate that the presence of ERα is required for the full execution of the response of the IGF-IR to IGF. In this respect, the presence of ERα, like COX-2/PG/nitric-oxide synthase/NO signaling, represents another "licensing factor" for IGF signaling.

ERα has been reported to bind IGF-IR directly and enable estrogen to activate IGF-IR (63, 65). That inhibition of ERK1/2 activation blocks ERα interaction with IGF-IR (63) suggests that the ERK family of mitogen-activated protein kinases is an essential prerequisite for ERα to activate IGF-IR. We have previously reported rapid phosphorylation of ERα by ERK1/2 following strain (99). However, this occurs far sooner than the activation of AKT. Bellido and coworkers (100) have proposed the existence of a strain-sensitive signalosome complex in osteocytes that consists of integrins, Src kinases, and ERKs. This functions basally to mediate signaling between the cells and their extracellular matrix to activate ERKs and promote cell survival. It also provides a strain-related mechanism to protect osteocytes from apoptosis (100). It is possible therefore that strain stimulates ERK-mediated phosphorylation of ERα in the very early stages of the strain response and that this phosphorylation status influences its ability to bind IGF-IR. Once bound to IGF-IR, ERα could then act to sensitize the cells to IGF signaling via PI3K/AKT. This would require the assembly of a large multiprotein complex that functions to promote ERα-dependent activation of IGF-IR. Interestingly, both Kahlert *et al.* (63) and Song *et al.* 101) describe the ability of E_2 to stimulate ERK activation via the interaction of ERα and IGF-IR, but we have not been able to reproduce this response in UMR-106 cells. Indeed, we show that E_2 inhibits its activation of AKT by des-(1–3)IGF-I in an ERα-dependent fashion. This may reflect a fundamental difference in the mechanism of cross-talk between ERα and IGF-1R between bone cells and cells in other tissues. In breast cancer cells, it is Shc-dependent shuttling of ERα to the membrane that juxtaposes ERα to IGF-IR. In osteoblasts, where ERK activation by strain has an absolute dependence on ERα membrane localization in a ligand-independent fashion (25), this is mediated by the interaction between caveolin 1 and ERα. The inhibitory effects of E_2 on des-(1–3)IGF-I-dependent activation of AKT we show here may be explained by our previous observation in osteoblasts that mechanical strain results in both the nuclear and membrane translocation of ERα, whereas the addition of E_2 results only in ERα nuclear localization (102). This suggests that a treatment such as E_2 that prevents membrane association of ERα would limit the ability of ERα to "license" IGF-I signaling. This provides a possible explanation for why under certain circumstances E_2 inhibits the adaptive response to mechanical strain (103, 104).

In summary, our *in vitro* experiments indicate that in primary cultures of mouse osteoblast-like cells, and cells of the UMR-106 osteoblastic cell line, a single short period of strain stimulates two phases of response, which are outlined in Fig. 8. In the first, strain stimulates ERα-related activation of IGF1R by ambient IGF followed by PI3K-mediated AKT phosphorylation/inhibition of GSK-3β and increased levels of active β-cate-

nin, which translocate to the nucleus and regulate Lef/TCF-mediated transcription. This early strain-responsive pathway is independent of the LRP5/6Frizzled/Wnt receptor pathway and does not require increased levels of ambient IGF. This pathway can be blocked at the level of AKT activation by inhibitors of COX-2/PG/nitric-oxide synthase/NO but cannot be mimicked by PG or NO individually. This suggests that a multiple key arrangement is necessary for the activation of this pathway and the existence of multiple strain-responsive pathways. In the second phase of the strain response, IGR-1R activation is stimulated by increased ambient IGF following strain-related, PG-mediated increase in IGF production. The existence of multiple pathways and the cross-talk between them will determine the strain-related outcome in terms of adaptive (re)modeling and local control of bone mass and architecture.

Acknowledgment—We thank Rosemary Suswillo for expert technical assistance.

REFERENCES

1. Klein-Nulend, J., van der Plas, A., Semeins, C. M., Ajubi, N. E., Frangos, J. A., Nijweide, P. J., and Burger, E. H. (1995) *FASEB J.* **9,** 441–445
2. Jessop, H. L., Rawlinson, S. C., Pitsillides, A. A., and Lanyon, L. E. (2002) *Bone* **31,** 186–194
3. Zaman, G., Suswillo, R. F., Cheng, M. Z., Tavares, I. A., and Lanyon, L. E. (1997) *J. Bone Miner. Res.* **12,** 769–777
4. Rawlinson, S. C., el-Haj, A. J., Minter, S. L., Tavares, I. A., Bennett, A., and Lanyon, L. E. (1991) *J. Bone Miner. Res.* **6,** 1345–1351
5. Li, J., Burr, D. B., and Turner, C. H. (2002) *Calcif. Tissue Int.* **70,** 320–329
6. Pitsillides, A. A., Rawlinson, S. C., Suswillo, R. F., Bourrin, S., Zaman, G., and Lanyon, L. E. (1995) *FASEB J.* **9,** 1614–1622
7. van't Hof, R. J., and Ralston, S. H. (2001) *Immunology* **103,** 255–261
8. Zaman, G., Pitsillides, A. A., Rawlinson, S. C., Suswillo, R. F., Mosley, J. R., Cheng, M. Z., Platts, L. A., Hukkanen, M., Polak, J. M., and Lanyon, L. E. (1999) *J. Bone Miner. Res.* **14,** 1123–1131
9. Armour, K. E., Armour, K. J., Gallagher, M. E., Gödecke, A., Helfrich, M. H., Reid, D. M., and Ralston, S. H. (2001) *Endocrinology* **142,** 760–766
10. Nakamura, E., Uezono, Y., Narusawa, K., Shibuya, I., Oishi, Y., Tanaka, M., Yanagihara, N., Nakamura, T., and Izumi, F. (2000) *Am. J. Physiol. Cell Physiol.* **279,** C510–C519
11. Costessi, A., Pines, A., D'Andrea, P., Romanello, M., Damante, G., Cesaratto, L., Quadrifoglio, F., Moro, L., and Tell, G. (2005) *Bone* **36,** 418–432
12. Monroe, J. J., and Tashjian, A. H., Jr. (1996) *Biochem. Biophys. Res. Commun.* **225,** 320–325
13. Genetos, D. C., Kephart, C. J., Zhang, Y., Yellowley, C. E., and Donahue, H. J. (2007) *J. Cell. Physiol.* **212,** 207–214
14. Armstrong, V. J., Muzylak, M., Sunters, A., Zaman, G., Saxon, L. K., Price, J. S., and Lanyon, L. E. (2007) *J. Biol. Chem.* **282,** 20715–20727
15. Lau, K. H., Kapur, S., Kesavan, C., and Baylink, D. J. (2006) *J. Biol. Chem.* **281,** 9576–9588
16. Westendorf, J. J., Kahler, R. A., and Schroeder, T. M. (2004) *Gene* **341,** 19–39
17. Robling, A. G., Niziolek, P. J., Baldridge, L. A., Condon, K. W., Allen, M. R., Alam, I., Mantila, S. M., Gluhak-Heinrich, J., Bellido, T. M., Harris, S. E., and Turner, C. H. (2008) *J. Biol. Chem.* **283,** 5866–5875
18. Cheng, M., Zaman, G., Rawlinson, S. C., Mohan, S., Baylink, D. J., and Lanyon, L. E. (1999) *J. Bone Miner. Res.* **14,** 1742–1750
19. Damien, E., Price, J. S., and Lanyon, L. E. (1998) *J. Bone Miner. Res.* **13,** 1275–1282
20. Damien, E., Price, J. S., and Lanyon, L. E. (2000) *J. Bone Miner. Res.* **15,** 2169–2177
21. Visconti, L. A., Yen, E. H., and Johnson, R. B. (2004) *Arch. Oral Biol.* **49,** 485–492
22. Lee, K. C., Jessop, H., Suswillo, R., Zaman, G., and Lanyon, L. E. (2004) *J. Endocrinol.* **182,** 193–201
23. Lee, K., Jessop, H., Suswillo, R., Zaman, G., and Lanyon, L. (2003) *Nature* **424,** 389
24. Jessop, H. L., Suswillo, R. F., Rawlinson, S. C., Zaman, G., Lee, K., Das-Gupta, V., Pitsillides, A. A., and Lanyon, L. E. (2004) *J. Bone Miner. Res.* **19,** 938–946
25. Aguirre, J. I., Plotkin, L. I., Gortazar, A. R., Millan, M. M., O'Brien, C. A., Manolagas, S. C., and Bellido, T. (2007) *J. Biol. Chem.* **282,** 25501–25508
26. Lanyon, L., Armstrong, V., Ong, D., Zaman, G., and Price, J. (2004) *J. Endocrinol.* **182,** 183–191
27. Bikle, D., Majumdar, S., Laib, A., Powell-Braxton, L., Rosen, C., Beamer, W., Nauman, E., Leary, C., and Halloran, B. (2001) *J. Bone Miner. Res.* **16,** 2320–2329
28. Wang, Y., Nishida, S., Sakata, T., Elalieh, H. Z., Chang, W., Halloran, B. P., Doty, S. B., and Bikle, D. D. (2006) *Endocrinology* **147,** 4753–4761
29. Liu, J. M., Zhao, H. Y., Ning, G., Chen, Y., Zhang, L. Z., Sun, L. H., Zhao, Y. J., Xu, M. Y., and Chen, J. L. (2008) *J. Bone Miner. Metab.* **26,** 159–164
30. Raab-Cullen, D. M., Thiede, M. A., Petersen, D. N., Kimmel, D. B., and Recker, R. R. (1994) *Calcif. Tissue Int.* **55,** 473–478
31. Lean, J. M., Jagger, C. J., Chambers, T. J., and Chow, J. W. (1995) *Am. J. Physiol.* **268,** E318–E327
32. Kawata, A., and Mikuni-Takagaki, Y. (1998) *Biochem. Biophys. Res. Commun.* **246,** 404–408
33. Kodama, Y., Umemura, Y., Nagasawa, S., Beamer, W. G., Donahue, L. R., Rosen, C. R., Baylink, D. J., and Farley, J. R. (2000) *Calcif. Tissue Int.* **66,** 298–306
34. Reijnders, C. M., Bravenboer, N., Tromp, A. M., Blankenstein, M. A., and Lips, P. (2007) *J. Endocrinol.* **192,** 131–140
35. Cheng, M. Z., Rawlinson, S. C., Pitsillides, A. A., Zaman, G., Mohan, S., Baylink, D. J., and Lanyon, L. E. (2002) *J. Bone Miner. Res.* **17,** 593–602
36. Topalli, I., and Etgen, A. M. (2004) *Brain Res.* **1030,** 116–124
37. Mendez, P., Wandosell, F., and Garcia-Segura, L. M. (2006) *Front. Neuroendocrinol.* **27,** 391–403
38. Mendez, P., Azcoitia, I., and Garcia-Segura, L. M. (2003) *Brain Res. Mol. Brain Res.* **112,** 170–176
39. Manning, B. D., and Cantley, L. C. (2007) *Cell* **129,** 1261–1274
40. Cantley, L. C., and Neel, B. G. (1999) *Proc. Natl. Acad. Sci. U.S.A.* **96,** 4240–4245
41. Campana, W. M., Darin, S. J., and O'Brien, J. S. (1999) *J. Neurosci. Res.* **57,** 332–341
42. Kawamura, N., Kugimiya, F., Oshima, Y., Ohba, S., Ikeda, T., Saito, T., Shinoda, Y., Kawasaki, Y., Ogata, N., Hoshi, K., Akiyama, T., Chen, W. S., Hay, N., Tobe, K., Kadowaki, T., Azuma, Y., Tanaka, S., Nakamura, K., Chung, U. I., and Kawaguchi, H. (2007) *PLoS ONE* **2,** e1058
43. Liu, X., Bruxvoort, K. J., Zylstra, C. R., Liu, J., Cichowski, R., Faugere, M. C., Bouxsein, M. L., Wan, C., Williams, B. O., and Clemens, T. L. (2007) *Proc. Natl. Acad. Sci. U.S.A.* **104,** 2259–2264
44. Dufour, C., Holy, X., and Marie, P. J. (2008) *Am. J. Physiol. Endocrinol. Metab.* **294,** E794–E801
45. Case, N., Ma, M., Sen, B., Xie, Z., Gross, T. S., and Rubin, J. (2008) *J. Biol. Chem.* **283,** 29196–29205
46. Pavalko, F. M., Gerard, R. L., Ponik, S. M., Gallagher, P. J., Jin, Y., and Norvell, S. M. (2003) *J. Cell. Physiol.* **194,** 194–205
47. Norvell, S. M., Alvarez, M., Bidwell, J. P., and Pavalko, F. M. (2004) *Calcif. Tissue Int.* **75,** 396–404
48. Naito, A. T., Akazawa, H., Takano, H., Minamino, T., Nagai, T., Aburatani, H., and Komuro, I. (2005) *Circ. Res.* **97,** 144–151
49. Desbois-Mouthon, C., Cadoret, A., Blivet-Van Eggelpoël, M. J., Bertrand, F., Cherqui, G., Perret, C., and Capeau, J. (2001) *Oncogene* **20,** 252–259
50. Smith, E., and Frenkel, B. (2005) *J. Biol. Chem.* **280,** 2388–2394
51. Campbell, R. A., Bhat-Nakshatri, P., Patel, N. M., Constantinidou, D., Ali, S., and Nakshatri, H. (2001) *J. Biol. Chem.* **276,** 9817–9824
52. Sun, M., Paciga, J. E., Feldman, R. I., Yuan, Z., Coppola, D., Lu, Y. Y., Shelley, S. A., Nicosia, S. V., and Cheng, J. Q. (2001) *Cancer Res.* **61,** 5985–5991
53. Vilgelm, A., Lian, Z., Wang, H., Beauparlant, S. L., Klein-Szanto, A., Ellenson, L. H., and Di Cristofano, A. (2006) *Cancer Res.* **66,** 3375–3380

54. Honda, K., Sawada, H., Kihara, T., Urushitani, M., Nakamizo, T., Akaike, A., and Shimohama, S. (2000) *J. Neurosci. Res.* **60,** 321–327
55. Alexaki, V. I., Charalampopoulos, I., Kampa, M., Vassalou, H., Theodoropoulos, P., Stathopoulos, E. N., Hatzoglou, A., Gravanis, A., and Castanas, E. (2004) *FASEB J.* **18,** 1594–1596
56. Mannella, P., and Brinton, R. D. (2006) *J. Neurosci.* **26,** 9439–9447
57. Zhang, S., Li, X., Burghardt, R., Smith, R., 3rd, and Safe, S. H. (2005) *J. Mol. Endocrinol.* **35,** 433–447
58. Ramaswamy, S., Nakamura, N., Vazquez, F., Batt, D. B., Perera, S., Roberts, T. M., and Sellers, W. R. (1999) *Proc. Natl. Acad. Sci. U.S.A.* **96,** 2110–2115
59. Krupnik, V. E., Sharp, J. D., Jiang, C., Robison, K., Chickering, T. W., Amaravadi, L., Brown, D. E., Guyot, D., Mays, G., Leiby, K., Chang, B., Duong, T., Goodearl, A. D., Gearing, D. P., Sokol, S. Y., and McCarthy, S. A. (1999) *Gene* **238,** 301–313
60. Kispert, A., Vainio, S., and McMahon, A. P. (1998) *Development* **125,** 4225–4234
61. Sunters, A., Thomas, D. P., Yeudall, W. A., and Grigoriadis, A. E. (2004) *J. Biol. Chem.* **279,** 9882–9891
62. Fermor, B., Gundle, R., Evans, M., Emerton, M., Pocock, A., and Murray, D. (1998) *Bone* **22,** 637–643
63. Kahlert, S., Nuedling, S., van Eickels, M., Vetter, H., Meyer, R., and Grohe, C. (2000) *J. Biol. Chem.* **275,** 18447–18453
64. Song, R. X., McPherson, R. A., Adam, L., Bao, Y., Shupnik, M., Kumar, R., and Santen, R. J. (2002) *Mol. Endocrinol.* **16,** 116–127
65. Song, R. X., Fan, P., Yue, W., Chen, Y., and Santen, R. J. (2006) *Endocr. Relat. Cancer* **13,** S3–S13
66. Hoyland, J. A., Mee, A. P., Baird, P., Braidman, I. P., Mawer, E. B., and Freemont, A. J. (1997) *Bone* **20,** 87–92
67. Colston, K. W., King, R. J., Hayward, J., Fraser, D. I., Horton, M. A., Stevenson, J. C., and Arnett, T. R. (1989) *J. Bone Miner. Res.* **4,** 625–631
68. Danciu, T. E., Adam, R. M., Naruse, K., Freeman, M. R., and Hauschka, P. V. (2003) *FEBS Lett.* **536,** 193–197
69. Ai, M., Heeger, S., Bartels, C. F., and Schelling, D. K. (2005) *Am. J. Hum. Genet.* **77,** 741–753
70. Babij, P., Zhao, W., Small, C., Kharode, Y., Yaworsky, P. J., Bouxsein, M. L., Reddy, P. S., Bodine, P. V., Robinson, J. A., Bhat, B., Marzolf, J., Moran, R. A., and Bex, F. (2003) *J. Bone Miner. Res.* **18,** 960–974
71. Gong, Y., Slee, R. B., Fukai, N., Rawadi, G., Roman-Roman, S., Reginato, A. M., Wang, H., Cundy, T., Glorieux, F. H., Lev, D., Zacharin, M., Oexle, K., Marcelino, J., Suwairi, W., Heeger, S., Sabatakos, G., Apte, S., Adkins, W. N., Allgrove, J., Arslan-Kirchner, M., Batch, J. A., Beighton, P., Black, G. C., Boles, R. G., Boon, L. M., Borrone, C., Brunner, H. G., Carle, G. F., Dallapiccola, B., De Paepe, A., Floege, B., Halfhide, M. L., Hall, B., Hennekam, R. C., Hirose, T., Jans, A., Jüppner, H., Kim, C. A., Keppler-Noreuil, K., Kohlschuetter, A., LaCombe, D., Lambert, M., Lemyre, E., Letteboer, T., Peltonen, L., Ramesar, R. S., Romanengo, M., Somer, H., Steichen-Gersdorf, E., Steinmann, B., Sullivan, B., Superti-Furga, A., Swoboda, W., van den Boogaard, M. J., Van Hul, W., Vikkula, M., Votruba, M., Zabel, B., Garcia, T., Baron, R., Olsen, B. R., and Warman, M. L. (2001) *Cell* **107,** 513–523
72. Ferrari, S. L., Deutsch, S., and Antonarakis, S. E. (2005) *Curr. Opin. Lipidol.* **16,** 207–214
73. Little, R. D., Carulli, J. P., Del Mastro, R. G., Dupuis, J., Osborne, M., Folz, C., Manning, S. P., Swain, P. M., Zhao, S. C., Eustace, B., Lappe, M. M., Spitzer, L., Zweier, S., Braunschweiger, K., Benchekroun, Y., Hu, X., Adair, R., Chee, L., FitzGerald, M. G., Tulig, C., Caruso, A., Tzellas, N., Bawa, A., Franklin, B., McGuire, S., Nogues, X., Gong, G., Allen, K. M., Anisowicz, A., Morales, A. J., Lomedico, P. T., Recker, S. M., Van Eerdewegh, P., Recker, R. R., and Johnson, M. L. (2002) *Am. J. Hum. Genet.* **70,** 11–19
74. Sawakami, K., Robling, A. G., Ai, M., Pitner, N. D., Liu, D., Warden, S. J., Li, J., Maye, P., Rowe, D. W., Duncan, R. L., Warman, M. L., and Turner, C. H. (2006) *J. Biol. Chem.* **281,** 23698–23711
75. Van Wesenbeeck, L., Cleiren, E., Gram, J., Beals, R. K., Bénichou, O., Scopelliti, D., Key, L., Renton, T., Bartels, C., Gong, Y., Warman, M. L., De Vernejoul, M. C., Bollerslev, J., and Van Hul, W. (2003) *Am. J. Hum. Genet.* **72,** 763–771
76. Fan, X., Rahnert, J. A., Murphy, T. C., Nanes, M. S., Greenfield, E. M., and Rubin, J. (2006) *J. Cell. Physiol.* **207,** 454–460
77. Chambers, T. J., Owens, J. M., Hattersley, G., Jat, P. S., and Noble, M. D. (1993) *Proc. Natl. Acad. Sci. U.S.A.* **90,** 5578–5582
78. Jat, P. S., Noble, M. D., Ataliotis, P., Tanaka, Y., Yannoutsos, N., Larsen, L., and Kioussis, D. (1991) *Proc. Natl. Acad. Sci. U.S.A.* **88,** 5096–5100
79. Noble, M., Groves, A. K., Ataliotis, P., Ikram, Z., and Jat, P. S. (1995) *Transgenic Res.* **4,** 215–225
80. Anitha, M., Joseph, I., Ding, X., Torre, E. R., Sawchuk, M. A., Mwangi, S., Hochman, S., Sitaraman, S. V., Anania, F., and Srinivasan, S. (2008) *Gastroenterology* **134,** 1424–1435
81. Cacciotti, P., Barbone, D., Porta, C., Altomare, D. A., Testa, J. R., Mutti, L., and Gaudino, G. (2005) *Cancer Res.* **65,** 5256–5262
82. DeAngelis, T., Chen, J., Wu, A., Prisco, M., and Baserga, R. (2006) *Oncogene* **25,** 32–42
83. Yu, Y., and Alwine, J. C. (2008) *J. Virol.* **82,** 4521–4526
84. Wu, X., Tu, X., Joeng, K. S., Hilton, M. J., Williams, D. A., and Long, F. (2008) *Cell* **133,** 340–353
85. Fang, D., Hawke, D., Zheng, Y., Xia, Y., Meisenhelder, J., Nika, H., Mills, G. B., Kobayashi, R., Hunter, T., and Lu, Z. (2007) *J. Biol. Chem.* **282,** 11221–11229
86. Johnson, D. L., McAllister, T. N., and Frangos, J. A. (1996) *Am. J. Physiol.* **271,** E205–E208
87. Binderman, I., Zor, U., Kaye, A. M., Shimshoni, Z., Harell, A., and Sömjen, D. (1988) *Calcif. Tissue Int.* **42,** 261–266
88. Tang, L. Y., Cullen, D. M., Yee, J. A., Jee, W. S., and Kimmel, D. B. (1997) *J. Bone Miner. Res.* **12,** 276–282
89. Pead, M. J., and Lanyon, L. E. (1989) *Calcif. Tissue Int.* **45,** 34–40
90. Dallas, S. L., Zaman, G., Pead, M. J., and Lanyon, L. E. (1993) *J. Bone Miner. Res.* **8,** 251–259
91. Chambers, T. J., Fox, S., Jagger, C. J., Lean, J. M., and Chow, J. W. (1999) *Osteoarthritis Cartilage* **7,** 422–423
92. Castellone, M. D., Teramoto, H., Williams, B. O., Druey, K. M., and Gutkind, J. S. (2005) *Science* **310,** 1504–1510
93. Chun, K. S., Akunda, J. K., and Langenbach, R. (2007) *Cancer Res.* **67,** 2015–2021
94. Namkoong, S., Lee, S. J., Kim, C. K., Kim, Y. M., Chung, H. T., Lee, H., Han, J. A., Ha, K. S., Kwon, Y. G., and Kim, Y. M. (2005) *Exp. Mol. Med.* **37,** 588–600
95. Prueitt, R. L., Boersma, B. J., Howe, T. M., Goodman, J. E., Thomas, D. D., Ying, L., Pfiester, C. M., Yfantis, H. G., Cottrell, J. R., Lee, D. H., Remaley, A. T., Hofseth, L. J., Wink, D. A., and Ambs, S. (2007) *Int. J. Cancer* **120,** 796–805
96. Tessner, T. G., Muhale, F., Riehl, T. E., Anant, S., and Stenson, W. F. (2004) *J. Clin. Invest.* **114,** 1676–1685
97. Wang, X., and Klein, R. D. (2007) *Mol. Carcinog.* **46,** 912–923
98. Klotz, D. M., Hewitt, S. C., Ciana, P., Raviscioni, M., Lindzey, J. K., Foley, J., Maggi, A., DiAugustine, R. P., and Korach, K. S. (2002) *J. Biol. Chem.* **277,** 8531–8537
99. Jessop, H. L., Sjöberg, M., Cheng, M. Z., Zaman, G., Wheeler-Jones, C. P., and Lanyon, L. E. (2001) *J. Bone Miner. Res.* **16,** 1045–1055
100. Plotkin, L. I., Mathov, I., Aguirre, J. I., Parfitt, A. M., Manolagas, S. C., and Bellido, T. (2005) *Am. J. Physiol. Cell Physiol.* **289,** C633–C643
101. Song, R. X., Barnes, C. J., Zhang, Z., Bao, Y., Kumar, R., and Santen, R. J. (2004) *Proc. Natl. Acad. Sci. U.S.A.* **101,** 2076–2081
102. Zaman, G., Jessop, H. L., Muzylak, M., De Souza, R. L., Pitsillides, A. A., Price, J. S., and Lanyon, L. L. (2006) *J. Bone Miner. Res.* **21,** 1297–1306
103. Saxon, L. K., and Turner, C. H. (2006) *Bone* **39,** 1261–1267
104. Jagger, C. J., Chow, J. W., and Chambers, T. J. (1996) *J. Clin. Invest.* **98,** 2351–2357